Applied Ocean Research 125 (2022) 103220

Contents lists available at ScienceDirect

Applied Ocean Research

journal homepage: www.elsevier.com/locate/apor

The effects of transitions in cover type and height on the wave overtopping load on grass-covered flood defences

Vera M. van Bergeijk [b,a], Jord J. Warmink [a,*], Suzanne J.M.H. Hulscher [a]

[a] Department of Marine and Fluvial Systems, University of Twente, Drienerlolaan 5, Enschede, 7522 NB, The Netherlands
[b] Department of Coastal Structures and Waves, Deltares, Boussinesqweg 1, Delft, 2629 HV, The Netherlands

ARTICLE INFO

Keywords:
Hydraulic forces
OpenFOAM
Erosion
Levee
Revetment
Transition

ABSTRACT

Grass cover erosion by overtopping waves is one of the main failure mechanisms of grass-covered flood defences. Observations have shown that grass cover erosion often starts at transitions such as changes in cover type and geometric changes. However, it is unclear how the effect of transitions on the overtopping load can be included in existing erosion models. In this study, the increase in load as the result of transitions in cover type and height are quantified using a numerical model in OpenFOAM®. The hydraulic load by overtopping waves is simulated for various transitions in cover type on the crest and a landward berm as well as height transitions on the crest and the slope. The model results show that transitions in cover type have a limited effect on the hydraulic load contrary to height transitions that lead to more than doubling of the hydraulic load. Formulations for the maximum shear stress and the maximum normal stress as result of height transitions are determined based on a fit through the model results. These formulations can be used to include the effects of height transitions in existing calculation methods for the erosion by overtopping waves and the safety assessment of flood defences.

1. Introduction

Flood defences protect coastal communities and low-lying areas against flooding from rivers and seas. During storm events, waves can overtop these flood defences leading to water volumes flowing over the crest and down along the landward slope. These overtopping waves exert a hydraulic load on the grass cover that can lead to erosion of the cover. Therefore, only a limited amount of wave overtopping is allowed (EurOtop Manual, 2018). Existing flood defences need to be reinforced due to higher design water levels as the result of sea level rise (Toimil et al., 2020) and increasing river discharges (Blöschl et al., 2019), and due to new insights into the failure process (Slomp et al., 2016). One way to finance these reinforcements is by incorporating additional functions into the flood defence to create a multi-functional flood defence (Voorendt, 2017). Here, the water-retaining function of the flood defence is combined with functions such as recreation, transportation, housing, agriculture, and nature, that can help both to co-fund the reinforcement and to improve the quality of the landscape (Van Loon-Steensma and Vellinga, 2014; Marijnissen et al., 2019). These multi-functional flood defences increase in the number of transitions on the flood defence.

Transitions are defined as any change in material and geometry of the flood defences, such as slope changes at the crest line and toe. This is especially the case for grass-covered flood defences where transitions are located at roads, paths, and damages to the grass cover. For example, a road or path consisting of other material than the dike cover is identified as a transition in cover type. Additionally, a transition in height occurs in case the cover types are not smoothly connected. Experiments (Steendam et al., 2014; Hoffmans et al., 2018; Van Hoven et al., 2013; Van Steeg et al., 2015), numerical simulations (Bomers et al., 2018) and field observations (Simm et al., 2017, 2021) have shown that erosion by overtopping waves often starts at transitions. Overtopping waves on the crest and the landward slope exert a high hydraulic load on the cover that starts to erode when the load exceeds the strength of the cover. Transitions increase the hydraulic load and possibly reduce the cover strength which both result in more erosion (Hoffmans et al., 2018). Additionally, transitions affect the hydraulic processes of the overtopping flow such as the deceleration of the wave due to an increase in bottom friction for rough cover types. Moreover, geometric transitions can lead to flow separation from the dike cover resulting in high hydraulic loads at the location of reattachment (Ponsioen et al., 2019; Van Bergeijk et al., 2022). It is crucial to include the effects of transitions in the existing calculations methods for the design and the safety assessment because the cover mainly fails at

* Corresponding author.
E-mail address: j.j.warmink@utwente.nl (J.J. Warmink).

https://doi.org/10.1016/j.apor.2022.103220
Received 8 December 2021; Received in revised form 18 May 2022; Accepted 25 May 2022
Available online 11 June 2022

transitions. Therefore, transitions are the critical elements with regards to the safety assessment (Van Steeg et al., 2015; Simm et al., 2021).

The hydraulic load by overtopping waves can be described using different hydraulic variables such as the flow velocity, the pressure, the shear stress and the normal stress. There are two models for grass cover erosion by overtopping waves that can include the effect of transitions: the empirical Cumulative Overload Method (COM) (Van Der Meer et al., 2010) and the analytical Grass-Erosion Model (GEM) (Van Bergeijk et al., 2021a). The COM is used in the safety assessment for wave overtopping in the Netherlands and approximates the amount of erosion using a damage number. The load is calculated using the flow velocity on the crest and three influence factors for transitions: an acceleration factor for the acceleration along the slope, a load factor α_M for the increase in load at transitions and a strength factor for the reduction in cover strength at transitions (Van Hoven et al., 2013). Theoretical formulas were derived to calculate the load factor, but these theoretical formulas result in a wide range of possible values (Van Hoven et al., 2013). The GEM calculates the erosion depth along the profile and the load is determined by the flow velocity in combination with a turbulence parameter ω. The effects of transitions can be included by locally increasing the turbulence parameter and reducing the cover strength in the model (Van Bergeijk et al., 2021a, 2019a). Additionally, the flow velocity in the GEM is calculated along the profile including the effects of slope changes and cover type (Van Bergeijk et al., 2019b). The main challenge is that the values of the load factor in the COM and the turbulence parameter in the GEM are either unknown or uncertain for transitions. Therefore, it remains unclear how to accurately account for transitions in existing calculation methods for the design and the assessment of flood defences for overtopping.

Wave overtopping field tests on grass-covered dikes have been performed using the wave overtopping simulator (Van Der Meer et al., 2007) in the Netherlands that were used to calibrate the load factor for transitions (Van Hoven et al., 2013; Steendam et al., 2014; Hoffmans et al., 2018). However, several problems arose out of these experiments on transitions. Firstly, experiments on similar transitions showed different results, and secondly, the transitions often failed as the result of secondary effects such as construction and maintenance issues (Van Steeg et al., 2015; Simm et al., 2017). Thirdly, transitions in the field are often a combination of both transitions in cover type and geometry, which makes it difficult to study the hydraulic processes separately. For example, flow separation from the asphalt path and reattachment to the grass cover was observed during an experiment with a biking path but it is unknown if the flow separation is the result of the height difference or the roughness difference between the grass cover and the asphalt cover (Van Hoven and Klerk, 2021). These problems lead to a large range of load factors for similar transitions that were calibrated using the observed erosion depths during the overtopping experiments (Peeters et al., 2012; Van Hoven et al., 2013; Van Hoven and Boers, 2019; Van Der Meer et al., 2015). Therefore, it remains a challenge to identify the important hydraulic processes, generalise the results and derive a representative load factor for transitions based on field tests and observations.

Another approach to study the wave overtopping load is the use of Computational Fluid Dynamics (CFD) models (Bomers et al., 2018; Van Bergeijk et al., 2020; Suzuki et al., 2020; Chen et al., 2021b; Barendse et al., 2022). For example, CFD models are used to simulate the overtopping flow over roughness elements on the waterside slope (Chen et al., 2021b; Jacobsen et al., 2017; Altomare et al., 2014; Jensen et al., 2014), the impact forces on a flood defence with a vertical wall on the crest (Jacobsen et al., 2018; De Finis et al., 2020; Molines et al., 2020) and on a person standing on the crest (Suzuki et al., 2020; Chen et al., 2021c). CFD models can provide insights into the hydraulic processes at transitions and can be used to study the effects of transitions in cover type and geometry separately. A case study of a wave overtopping field test has previously been performed using a CFD model (Bomers et al., 2018) with a road on top of a grass-covered dike. This study mainly focused on the increase in cover erosion due to transitions and not specifically on the load. Thus, the model output was limited to the flow velocity and the flow separation process was not simulated. Although the study showed that the transitions in geometry and cover type increase the erosion, the results are specific for the simulated experiment and are therefore not directly applicable to include transitions in calculation methods for the design and the assessment of flood defences.

The goal of this study is to quantify the effects of transitions in cover type and in height on the overtopping load and determine the important hydraulic processes at these transitions. A numerical CFD model (Van Bergeijk et al., 2022, 2020) is used to calculate the hydraulic load on the cover along the crest and the landward slope expressed in the flow velocity, the pressure, the shear stress and the normal stress. The effects of transitions in cover type and height are studied separately as well as a combination of transitions in height and cover type. Firstly, the hydraulic processes at the transitions are studied such as the acceleration and the deceleration of the overtopping wave due to transitions in cover type or the flow separation at height transitions. These processes affect the spatial variation of the hydraulic variables and can thereby change the location of maximum load where most erosion is expected. Understanding the hydraulic processes at transitions and how they affect the spatial variation in the hydraulic load is important to predict the location of maximum hydraulic load and cover failure. Secondly, an engineering approach is followed to quantify the increase in load at transitions in terms of the flow velocity, the shear stress, the normal stress and the pressure. Relations for the shear stress and the normal stress at height transitions on the crest and the slope are developed using the numerical model output. These relations are a first step to describe the load at height transitions in existing calculation methods for wave overtopping erosion, such as the COM and the GEM, so that the effect of transitions can be included in the safety assessment for wave overtopping.

This paper is organised as follows: Section 2 describes observations of the load at transitions. Furthermore, the set-up of the numerical model and the modelled transitions are described followed by a method for the quantification of the load at transitions. Section 3 shows the model results and the practical implications of the effects of transitions on the hydraulic load are described in Section 4. Section 5 contains the discussion and the conclusions are drawn in Section 6.

2. Method

Transitions in cover type and height are simulated in a numerical model to determine the hydraulic load along the crest and the landward slope. Firstly, this section describes how transitions in cover type and geometry affect the hydraulic load based on observations during previous field experiments and in model simulations. Next, the numerical model set-up and the modelled transitions are described. The hydraulic processes at transitions are investigated by determining changes in the cross-dike variation of the hydraulic load. The load at the transitions is quantified using the numerical model output and compared to the results of analytical models. Finally, relations for the shear stress and the normal stress due to height transitions are derived and compared to descriptions of the load in existing calculation methods.

2.1. Observations at transitions

This study focuses on transitions that are uniform in the along-dike direction (Fig. 1a). Every flood defence includes transitions in geometry as the slope changes from the crest to the slope (I), and at the toes of the structure (II, III). The lower waterside slope of coastal dikes is often covered in a hard revetment to protect the cover and the core against the wave forces, while the upper waterside slope, the crest and the landward slope are covered in grass. This results in a transition in cover type (III), similar to roads that are often located on

Fig. 1. (a) A photo indicating transitions in cover type (II, III, IV), height (IV) and slope (I, II, III) on a grass-covered flood defence with roads on the crest and at the landward toe located at the Wadden Sea in the Netherlands. (b) Photo of a damage resulting in a small cliff (Bakker et al., 2008). (c) Dike cover erosion on the landward slope during wave overtopping field tests in the Netherlands.
Source: Photo by Juan Pablo Aguilar Lopez.

the crest, or on a berm on the slope (II, IV). At these transitions in cover type, transitions in height (IV) can occur when the cover types are not smoothly connected on an equal height level.

Transitions in geometry and cover type affect the hydraulic load of overtopping waves, and thereby the resulting cover erosion and cover failure (Morris et al., 2014; Steendam et al., 2014; Warmink et al., 2020). The load on the cover increases at the transition from a smooth to a rough bed where the roughness differences at the transitions in cover type can create additional turbulence (Van Hoven et al., 2013; Nezu and Nakagawa, 1993). For example, asphalt is smoother than grass so when the flow is directed from the road to the grass cover, the load increases and more erosion is expected (Bomers et al., 2018). Roughness transitions also affect the duration of the overtopping wave and thereby the amount of erosion (Bomers et al., 2018; Van Bergeijk et al., 2020), where a longer duration results in more erosion (Dean et al., 2010; Hoffmans, 2012).

At geometric transitions, the load increases as the result of jet impact (Hoffmans, 2012; Jorissen and Vrijling, 1989). At the toe, where the slope transits to a horizontal plane, the flow in the downward direction results in an impact area where energy is dissipated and a scour hole can form (Steendam et al., 2014). For steep slopes, the overtopping flow separates at the crest line and reattaches on the upper slope resulting in high impact forces (Van Damme et al., 2016; Ponsioen et al., 2019; Van Bergeijk et al., 2022). A similar process of flow separation and impact occurs at height transitions with a vertical drop such as cover damages and erosion holes (Van Bergeijk et al., 2021a) (Fig. 1b,c). A vertical rise in the profile results in impact against the height transition and the flow sweeps up into the air, similar to the wave overtopping process on a flood defence with a vertical wall on the crest (Jacobsen et al., 2018; De Finis et al., 2020; Molines et al., 2020). The wall experiences high normal forces and pressures, that could lead to structural failure or erosion. On the other hand, water collects in front of the wall that can lead to energy dissipation and damping of the wave forces (Hoffmans and Verheij, 2011; Bakker et al., 2013), and thereby reducing the load on the cover.

2.2. Numerical model setup

A numerical CFD model is used to calculate the hydraulic load by overtopping waves on the cover. The model simulates the 2D-vertical flow of one overtopping wave over the crest and the landward slope of grass-covered flood defences. The model is built in the open-source software OpenFOAM® version v2012 that solves the two-phase Reynolds-Averaged Navier–Stokes equations using the finite volume method. The model set-up of Van Bergeijk et al. (2022) is used in this study since this numerical model is the only model that proved able to simulate the flow separation and impact at geometric transitions. The model developed by Van Bergeijk et al. (2022) has previously been used to study the hydraulic processes and the load at slope changes. The model domain is adapted in this study for transitions in cover type and in height.

The model domain of the reference case without transitions has a crest height of 8 m, a crest width of 7 m, a slope steepness of 1:2.7 and a slope length of 18 m (Fig. 2a). The model domain continues 2 m behind the landward toe and both water and air can flow freely out of the domain. Height transitions are considered by adapting the model grid (Figs. 2b and 2c) as described in Section 2.3. The grid size is set to 1 cm x 1 cm (cross-dike Δx x vertical Δz) which is sufficiently small to accurately simulate the flow separation and impact process at height transitions (Van Bergeijk et al., 2022).

The model domain starts on the crest where the boundary conditions are generated using the overtopping volume V [m^3/m] to obtain the flow velocity $u_0(t)$ [m/s] and layer thickness $h_0(t)$ [m] as function of time (Van Der Meer et al., 2010; Hughes and Shaw, 2011)

$$u_0(t) = 4.5\,V^{0.34}\left(1-\frac{t}{T_0}\right) \quad \text{and} \quad h_0(t) = 0.133\,V^{0.5}\left(1-\frac{t}{T_0}\right). \tag{1}$$

with the time t and overtopping duration T_0 (Van Der Meer et al., 2010).

$$T_0 = 4.4V^{0.3} \tag{2}$$

The overtopping volumes simulated in this study vary between 0.6 m^3/m and 4.0 m^3/m. The smallest overtopping volume of 0.6 m^3/m is used in the simulations of transitions in cover type since changes in the bed roughness have a relative large effect on smaller volumes due to the small layer thickness. Previous studies (Ponsioen et al., 2019; Van Bergeijk et al., 2022) have indicated that flow separation at geometric transitions occurs for larger overtopping volumes and therefore the overtopping volume is increased up to 4.0 m^3/m for the simulations with height transitions. For the majority of the simulations, a volume of 2.0 m^3/m was used. This is the maximum overtopping volume that is expected for a significant wave height H_s of 1 m while this is a relative small overtopping volume for H_s = 3 m (EurOtop Manual, 2018).

The turbulence is solved using a $k-\omega$ SST turbulence mode, where SST stands for shear stress transport and the symbols correspond to the turbulent kinetic energy k [J/kg] and the specific rate of dissipation ω [1/s]. A wall function was used to include the effects of cover roughness in the turbulence model (OpenCFD Ltd, 2019). The roughness wall function for the kinematic viscosity ν requires a roughness constant C_s [–] and a Nikuradse roughness height K_s [m]. The roughness constant C_s describes the shape and the spacing of the roughness elements and is set to the default value of 0.5 (Nikuradse, 1950). The Nikuradse roughness height K_s describes the height of the roughness elements and is set to 8 mm for the grass cover based on calibration by Van Bergeijk et al. (2020). Transitions in cover types are represented by variations in roughness height K_s (Section 2.3).

The model calculates the flow velocity $u(x,t)$ [m/s], the pressure $p(x,t)$ [kPa], the shear stress $\tau_s(x,t)$ [kN/m^2] parallel to the profile and the normal stress $\tau_n(x,t)$ [kN/m^2] perpendicular to the profile as function of cross-dike location x and time t. The flow velocity, the shear stress, the normal stress and the pressure are multiplied by the

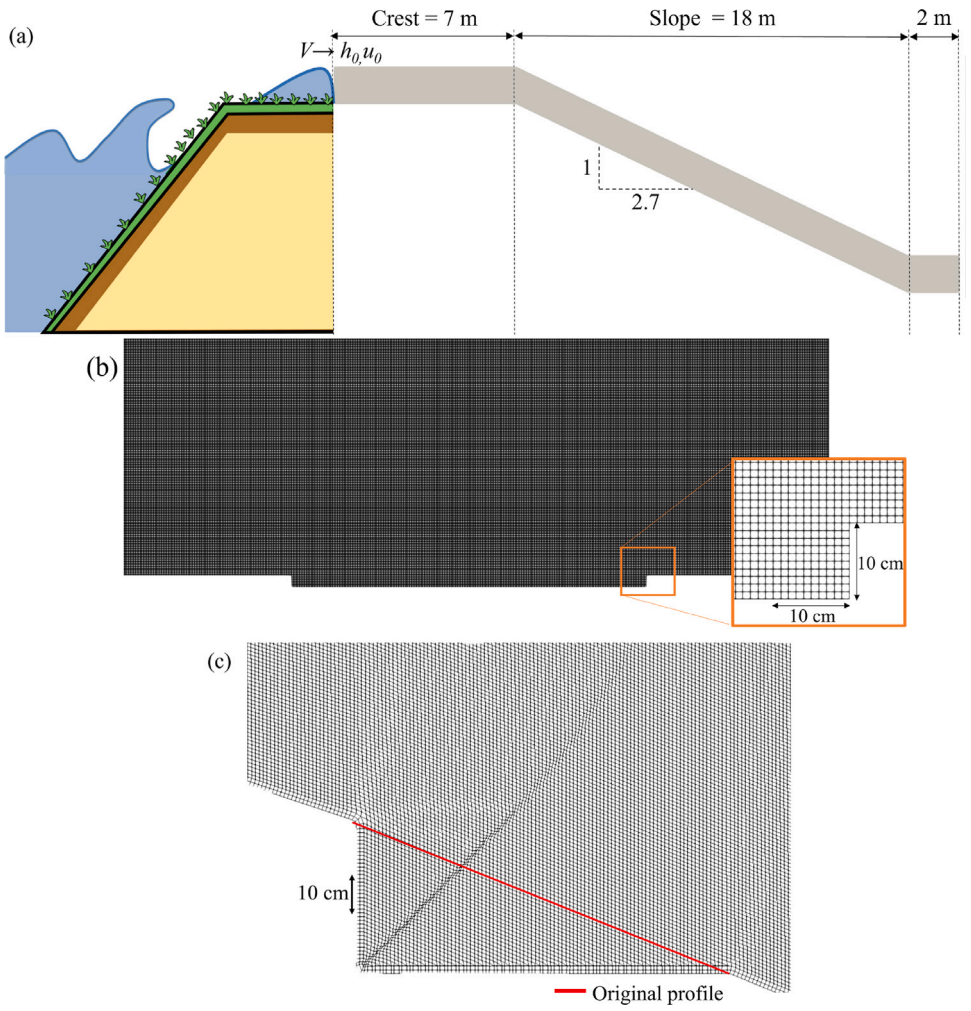

Fig. 2. (a) Schematisation of the model domain for the reference case. The model domain starts on the crest where the overtopping volume V is translated to the flow velocity u_0 and layer thickness h_0 that are used as boundary conditions in the model. (b) A close up of the grid at the height transitions on the crest. (b) A close up of the grid at the height transition on the slope representative for an erosion hole where the red line indicates the original profile.

water fraction, which is 0 for air, 1 for water and between 0 and 1 for air–water mixtures. The flow velocity is determined with a spacing of 0.5 m along the profile, while the other output variables are determined with a spacing of 1 cm for every boundary cell along the profile. The output is saved with 100 Hz which is necessary to accurately capture the impact forces at height transitions (Van Bergeijk et al., 2022).

2.3. Modelled transitions

For this study, we focus on longitudinal transitions that are uniform in the along dike direction (Fig. 1). Transitions in cover type and transitions in height are simulated using the numerical model. The locations of the modelled transitions along the profile are summarised in Fig. 3 and an overview of the model runs is provided in Table 2 and Appendix A.

Transitions in cover type are simulated by adapting the Nikuradse roughness height. The roughness of the cover can be expressed using the friction factor f [–], the Manning's coefficient n [s/m$^{1/3}$] or the Nikuradse roughness height K_s that are related as

$$f = \frac{2\,gn^2}{h^{1/3}} = \frac{K_s^{1/3}}{32h^{1/3}} \tag{3}$$

with the gravitational acceleration g and the layer thickness h. Van Bergeijk et al. (2020) calibrated a roughness height K_s of 8 mm for grass, while the friction coefficient f was calibrated to 0.01 by SBW (2012). These values coincide for a layer thickness of 20 cm (Table 1).

Table 1
Comparison of the Nikuradse roughness height K_s, the Manning's coefficient n and the friction factor f for the 5 simulated cover types using a layer thickness of 20 cm (Eq. (3)).

K_s [mm]	1	4.7	8	10	16
n [–]	0.0124	0.0160	0.0175	0.0181	0.0196
f [–]	0.005	0.009	0.010	0.011	0.013

Transitions in cover type are modelled on the crest and the berm of a grass-covered flood defence (Fig. 3). The transition is representative of a road that is located on the crest or the berm with a width of 3 m, similar to the dimensions of a road that was tested during a wave overtopping field test (Bakker et al., 2013). Four cover types are simulated with a roughness height of 1 mm, 4.7 mm, 10 mm and 16 mm. These values are representative for common cover types: cement (K_s = 1 mm), asphalt (K_s = 4.7 mm) and (smooth) earth (K_s = 10–16 mm) (Chow, 1959). In total, 15 model runs are performed to study transitions in cover type including the completely grass-covered reference case and the completely grass-covered berm case (Tables 2 and A.5).

The grid of the numerical model is adapted to simulate transitions in height. Two types of height transitions are simulated: height transitions on the crest and height transitions on the slope (Fig. 3, Table 2). A road on the crest is often located lower or higher compared to the grass cover, which is simulated by the height transitions on the crest. The height transitions on the slope are representative for erosion holes or

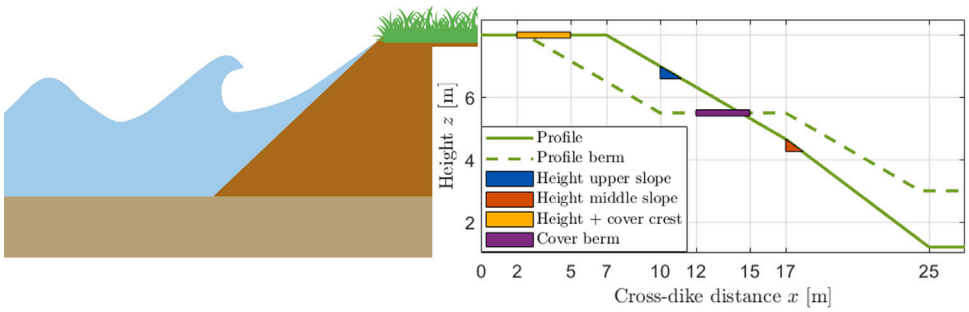

Fig. 3. The profiles of the reference case without transitions (green) and the berm case without transitions in cover type (green dashed) together with the locations of the transitions in cover type on the crest and the berm and the transitions in height on the crest and the slope.

Table 2
Overview of the modelled transitions. A full overview of the model simulations is provided in Appendix A.

Transition	Location	Variation	Runs
Cover	Crest	$K_s = 1, 4.7, 8, 10, 16$ mm	10
	Berm	$K_s = 1, 4.7, 8, 10, 16$ mm	5
Height	Crest	$d = -25, -10, -5, 5, 10, 25$ cm	10
	Slope	$d = 20, 40, 60, 80, 100$ cm	30
Cover + Height	Crest	$K_s = 4.7, 16$ mm, $d = -10, 10$ cm	4

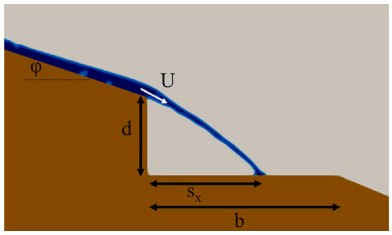

Fig. 4. Flow separation of a wave with flow velocity U at an erosion hole with height d, length b and slope angle φ that reattaches to the cover at the impact location s_x.

other type of damages resulting in a vertical cliff (Figs. 1c, 1d and 4). Fig. 2 shows a close up of the grid at the height transitions. The height transitions on the crest are created in the background mesh using the blockMesh utility (Fig. 2b). The grid for the height transitions on the slope required more modifications because the grid cells on the slope are lined up parallel to the slope. The erosion holes on the slope are cut out of the background mesh (red line) using the snappyHexMesh utility (OpenCFD Ltd, 2019) and 5 parallel layers to the profile were added to ensure that the hydraulic load on the cover is simulated properly (Fig. 2c). Although this method creates a small disturbance in the mesh further from the surface, the simulations of the load are more accurate compared to a case without parallel layers. In that case, the grid cells on the surface become irregularly shaped which significantly affects the simulated load (Van Bergeijk et al., 2021b).

Height transitions on the slope are modelled on the upper slope (x = 10 m) and the middle slope (x = 17 m) (Fig. 3) with a height d [m] varying between 0.2 m and 1.0 m (Fig. 4) and 5 overtopping volumes (V = 1–4 m^3/m) resulting in 30 runs (Table 2). These height transitions on the slope are representative for damages to the cover. Initial damages to the grass cover have a depth of around 20 cm as the result of roll-up or bulging, where the grass mat is cut and pushed up gradually (Hewlett et al., 1987). The cover material often has a thickness of around 1 m and therefore transitions with a height of 0.2–1.0 m are simulated.

The height transitions on the crest result in both vertical rises and vertical drops. These transitions are representative for the height differences between the asphalt and grass cover at a road, which is typically around 5–10 cm (Van Hoven et al., 2013). A more extreme height difference of 25 cm is also simulated resulting in 10 model simulations for height transitions on the crest.

Additionally, the combination of transitions and cover type are calculated for the crest (Table 2). Combinations of transitions with heights of 10 cm and -10 cm and cover types with K_s = 4.7 mm and K_s = 16 mm are simulated to investigate the effect of both transitions simultaneously and to determine the relative effect of both transitions.

2.4. Hydraulic processes

The effect of transitions on the cross-dike variation in the load along the crest and the landward slope is investigated to determine how transitions affect the location of the maximum load. The hydraulic load resulting in cover erosion can be separated into two loading mechanisms: shear loading and normal loading. Shear loading is the result of high flow velocities and turbulence and is expressed in the flow velocity and shear stress. Normal loading is the result of high impact forces due to flow separation and can be expressed in the normal stress and the pressure. Transitions in cover type lead to acceleration or deceleration of the overtopping wave and can thereby change the location of maximum flow velocity and thus shear loading. Previous studies have indicated that geometric transitions can influence both shear loading and normal loading (Steendam et al., 2014; Ponsioen et al., 2019; Van Bergeijk et al., 2022). For example, the slope change at the landward toe affects shear loading by increasing the flow velocity and turbulence leading to a maximum shear load around 0.5–1 m landward of the toe (Van Bergeijk et al., 2022; Steendam et al., 2014). The slope change at the landward crest line can result in flow separation for steep slopes in combination with larger overtopping volumes that leads to high normal loads on the upper slope (Van Bergeijk et al., 2022; Ponsioen et al., 2019). In this study, the acceleration and deceleration as the result of transitions in cover type is investigated by studying the flow velocity. Additionally, the variation of the shear stress along the profile is investigated to determine how transitions in cover type affect shear loading.

Since height transitions can affect both shear and normal loading, the variation in the four hydraulic variables along the dike is investigated: the maximum flow velocity $U(x)$, the maximum shear stress $T_s(x)$, the maximum normal stress $T_n(x)$ and the maximum pressure $P(x)$ with respect to time. The location of maximum load is determined for all four variables and the flow of the overtopping wave over the height transitions is observed to see if flow separation and impact occurs.

2.5. Quantifying the load at transitions

Next, the maximum hydraulic load at the transitions is quantified using the four hydraulic variables $U(x)$, $T_s(x)$, $T_n(x)$ and $P(x)$. The effect of transitions on the hydraulic load is investigated by comparing the modelled load of the reference case without transitions to the model runs with transitions (Fig. 3). The effect of transitions on these

hydraulic variables ζ ($\zeta = U, T_s, T_n, P$) is expressed as a percentage compared to the reference case without a transition ζ_{ref}.

$$\Delta\zeta = \frac{\max(\zeta(b)) - \max(\zeta_{ref}(b))}{\max(\zeta_{ref}(b))} \cdot 100\% \quad (4)$$

The maximum load as the result of a transition is often located downstream of the transition and not at the transitions itself as shown for the landward crest line and landward toe by Van Bergeijk et al. (2022). Therefore, the maximum load over a distance b is used to quantify the effect of the transition. This distance b is either the crest width (x = 0–7 m), berm width (x = 10–17 m) or the cross-dike length of the hole for transitions on the slope (Fig. 4).

2.5.1. Comparison to analytical models

It is important to be able to predict the maximum hydraulic load as the result of a transition, for example to calculate the amount of cover erosion. Numerical CFD models are computationally expensive and therefore less suitable to calculate the amount of erosion during a storm event. Therefore, analytical and empirical models are preferred to predict the hydraulic loads of overtopping waves. An analytical model for the flow velocity along a dike profile for various cover types and landward geometries was developed by Van Bergeijk et al. (2019b) Appendix B.1. The flow velocities of the numerical model are compared to the analytical model of Van Bergeijk et al. (2019b) to determine if this analytical model can be used to predict the effect of transitions on the hydraulic load.

Van Bergeijk et al. (2019b) derived analytical formulas from the 1D shallow water equations including the deceleration of the overtopping wave due to bottom friction and the acceleration of the wave along the slope due to gravitational acceleration. These formulas for horizontal parts (crest, berm) and for slopes are coupled in an analytical model that can account for the effects of transitions in cover type and slope changes on the flow velocity using the friction factor f and the slope angle φ. The analytical model is used to calculate the maximum flow velocity $U_a(x)$ along the crest, the slopes and the berm for the transitions in cover type using the friction factors in Table 1. Comparison between the flow velocity calculated with numerical model and the analytical model can indicate if the current version of the analytical model is able to describe the effect of transitions in cover type on the flow velocity, or an additional multiplication factor is necessary to account for effects that are not captured in this analytical model.

The accuracy of the analytical model is determined using the Nash–Sutcliffe efficiency factor NSE (Nash and Sutcliffe, 1970), which is calculated as

$$NSE = 1 - \frac{\sum_{i=1}^{N}(\zeta^*_{A,i} - \zeta^*_{m,i})^2}{\sum_{i=1}^{N}(\zeta^*_{m,i} - \overline{\zeta^*_m})^2} \quad (5)$$

with the number of runs N, the value during run i of the analytical model $\zeta^*_{A,i}$ or the numerical model $\zeta^*_{m,i}$ and the average of all model runs $\overline{\zeta^*_m}$. A perfect fit between the model results and the formulation results in a NSE of 1 and a NSE of 0 indicates that the formulation is as accurate as the mean of the model results.

The NSE of the analytical model for the flow velocity is calculated using the flow velocity $\zeta = U$ at the transitions in cover type at x = 2 m and x = 5 m on the crest for V = 0.6 m^3/m and V = 2.0 m^3/m. For the berm, the flow velocity at the transition in cover type at x = 12 m and x = 15 m for V = 2.0 m^3/m is used. The model results are compared for the 5 roughness heights (Table 2) resulting in 15 model runs to calculate the NSE.

Additionally, an analytical impact model was developed by Van Bergeijk et al. (2021b) to calculate the impact location s_x [m] as the result of a height transition with a vertical drop Appendix B.2. The impact location is calculated using the basic formulas for the trajectory of a projectile, the flow velocity before wave separation, the height of the transition and the slope angle φ (Fig. 4). The impact location is calculated for the height transitions using the analytical impact model $s_{x,A}$. The performance of the analytical impact model is determined using the NSE for the impact location, where the impact location in the OpenFOAM® model $s_{x,OF}$ is defined as the location of the maximum normal stress on the crest or the length of the hole b. For the transitions on the slope, the slope angle φ was used to calculate the impact location. An angle of 10° was used for the height transitions on the crest based on the observed angle of the flow at the location of flow separation in the numerical model. The simulations with transitions in height on the crest, the slope and the combination with transitions in cover type are used to calculate the NSE with a total of 44 runs (Table 2).

2.5.2. Relations for the shear stress and the normal stress

Currently, the COM and the GEM are the only models for wave overtopping that account for transitions in the description for the load. In both models, the increase in load at transitions is incorporated using a multiplication factor for the flow velocity Appendix B. The COM uses the load factor α_M varying between 1 and 2 to describe the increase in load at transitions. The GEM includes a turbulence parameter ω to account for the effect of turbulence on the erosion that can be used to describe the additional load on the cover due to transitions (Van Bergeijk et al., 2021a). The load factor α_M is unknown for height transitions and the turbulence parameter ω for a height transition is limited to a height of 20 cm (Van Bergeijk et al., 2021a).

Therefore, relations for the shear stress and the normal stress at height transitions are derived using the numerical model that can be used as a first step to calculate the load in erosion models. Since both the GEM and the COM use a multiplication factor for the flow velocity to describe the load at transitions, a relation for the stress as function of the flow velocity is desired. The relations for the maximum shear stress and the maximum normal stress as the result of height transitions are derived using a regression analysis. Next to the flow velocity, the load is expected to depend on the height of the transition d as jet impact simulations on grass covers have shown that the load increases with the height (Stanczak, 2008; Scheres and Schüttrumpf, 2020). The regression analysis is performed separately for the transitions on the slope and the transitions on the crest resulting in two formulas for the shear stress and two formulas for the normal stress. Different relations for the stresses are expected since the transitions on the slope only result in a vertical drop while the transitions on the crest include both a vertical drop and a vertical rise.

The dependency of the stress on the flow velocity is firstly determined during the regression analysis where it is expected that the stress increases with increasing flow velocity. Next, the relation between the height of the transition and the stress is determined in the regression analysis. These relations are based on the best fit through the model results and the accuracy of the relations is scored using the NSE described in Eq. (5) with $\zeta^*_{A,i}$ the value of the fit.

Finally, the relations are translated to the load factor α_M and the turbulence parameter ω to show how these relations can be used in existing calculation methods in Section 4. Additionally, the load factor and the turbulence parameter calculated using the numerical model results are compared to the theoretical and the calibrated values in Table B.6.

3. Model results

3.1. Transitions in cover type

3.1.1. Hydraulic processes

The maximum flow velocity increases at the transition from a rough to a smoother cover, for example grass (green) to K_s = 1 mm (blue-dashed) at x = 2 m, and decreases from a smooth to rougher cover, for example grass (green) to K_s = 16 mm (purple circles) at x = 2 m (Fig. 5). The change in flow velocity is larger for K_s = 1 mm

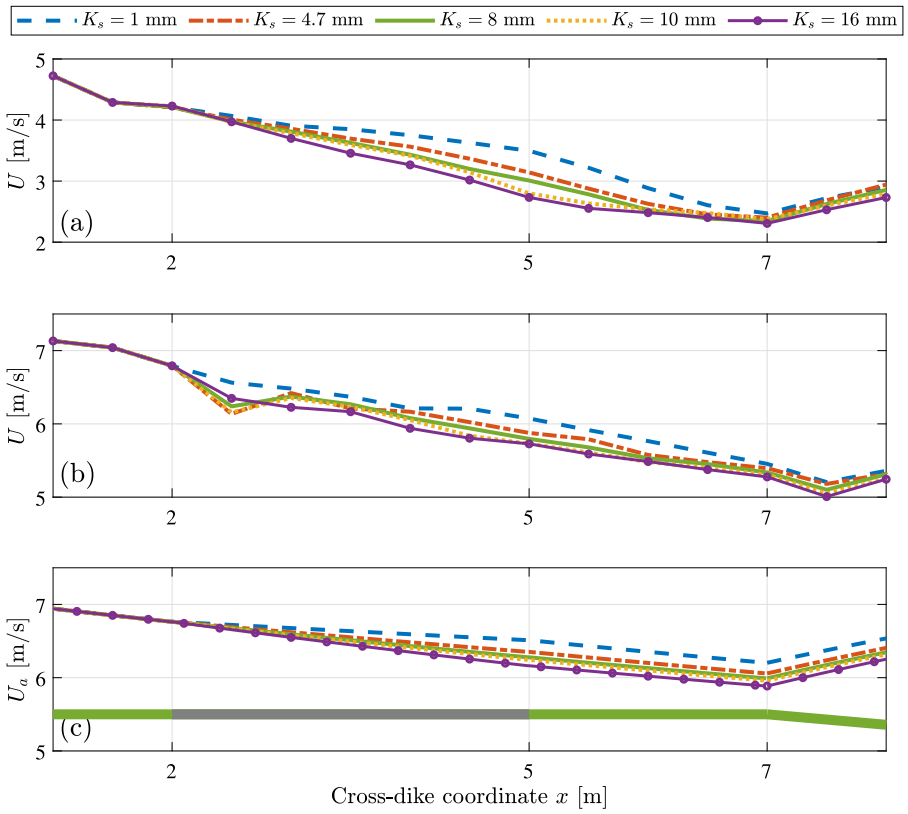

Fig. 5. The maximum flow velocity along the profile for transitions in cover type on the crest between grass (green, K_s = 8 mm) and another cover type with a Nikuradse roughness height K_s (grey) for: (a) the numerical model and V = 6.0 m^3/m, (b) the numerical model and V = 2.0 m^3/m, (c) the analytical model and V = 2.0 m^3/m,.

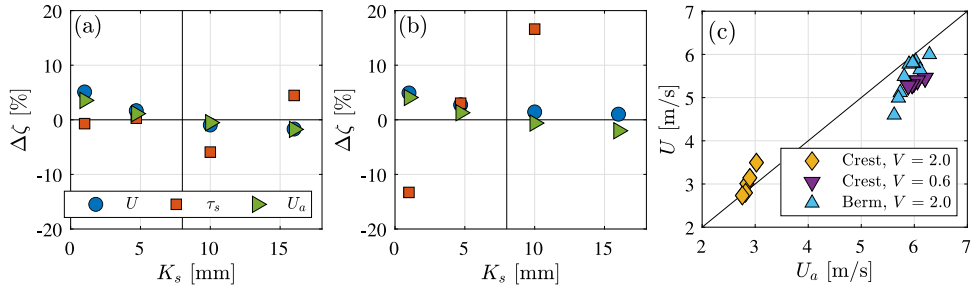

Fig. 6. (a) The increase in load for transitions in cover type on the crest with a roughness height K_s compared to the reference case without transitions and a grass cover (K_s = 8 mm) for V = 2.0 m^3/m. (b) The increase in load for transitions in cover type on the berm with a roughness height K_s compared to the reference case without transitions and a grass cover (K_s = 8 mm) for V = 2.0 m^3/m. (c) Comparison between the modelled flow velocities in the analytical model U_a and the numerical model U with an NSE of 0.89.

compared to K_s = 16 mm, which could be the result of the non-linear relationship between the Nikuradse roughness height K_s, the Mannings coefficient n and the friction factor f (Table 1) where the roughness difference between 16 mm and 8 mm is smaller compared to 1 mm and 8 mm for the Mannings coefficient and the friction factor. The effect of the transition on flow velocity depends on the overtopping volume. For small overtopping volumes, the layer thickness is small so the roughness of the revetment has relatively more effect compared to larger layer thicknesses for larger overtopping volumes. This results in difference of around 0.75 m/s between the different cover types at x = 5 m for V = 0.6 m^3/m (Fig. 5a) compared to 0.25 m/s for V = 2.0 m^3/m (Fig. 5b). The maximum difference of 0.75 m/s is the same order of magnitude as the measurement error of flow velocities (around 0.5 m/s) during field experiments (Van Hoven et al., 2013; Heida, 2021) which shows that transitions in cover type have a limited effect on the flow velocity.

Next to the flow velocity, the transitions in cover type have a limited effect on the shear stress with a maximum increase in load of 20% (Fig. 6). The differences in the shear stress are mainly related to the timing of the wave front. A rougher cover results in more bottom friction and thereby decelerates the flow while a smoother cover results in acceleration of the wave front. This is illustrated in the shear stress on the slope (Fig. 7) where a rough cover on the crest (K_s = 10 mm) results in the signal shifting towards the crest due to the deceleration, while the opposite happens in case of a smoother cover (K_s = 4.7 mm). This is in agreement with previous model studies that showed that the overtopping duration increases with the roughness height (Bomers et al., 2018; Van Bergeijk et al., 2020).

3.1.2. Comparison to the analytical model

The analytical model of Van Bergeijk et al. (2019b) is able to predict the maximum flow velocity over the crest with a transition in cover type with a NSE of 0.88 (Figs. 5c and 6c). The analytical model calculates a smaller flow velocity for the larger overtopping volume of V = 2.0 m^3/m. This might be the result of a difference in the

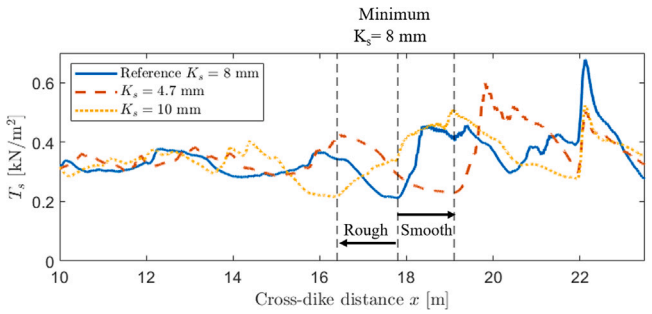

Fig. 7. The maximum shear stress $T_s(x)$ on the slope in case of transition in cover type on the crest with a roughness K_s compared to the reference case. The dashed lines indicate the location of the minimum in T_s that is shifted towards the crest for a transition with a rough cover (K_s = 10 mm) and towards the landward toe for a smooth cover (K_s = 4.7 mm).

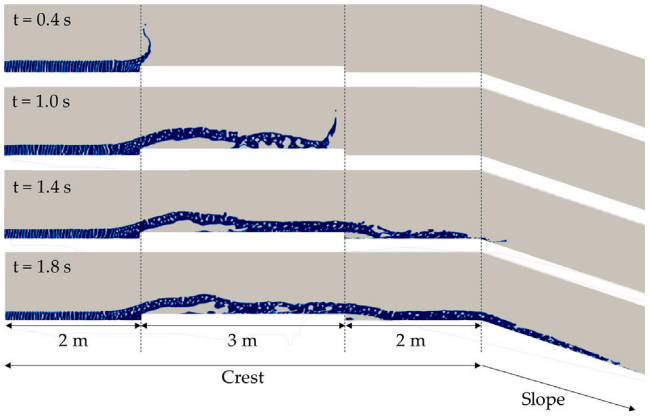

Fig. 8. Screenshots of the overtopping flow at time t for height transitions on the crest with a height of 10 cm above the crest level ($H8$).

boundary conditions since the analytical model predicts a smaller flow velocity in both the front of and behind the transition. The analytical model solely uses the maximum layer thickness and the maximum flow velocity as boundary condition, while the numerical model also includes information over time based on the overtopping duration. Although the analytical model slightly under predicts the magnitude of the maximum flow velocity, it predicts a similar relative change in the flow velocity ΔU for the transition on the crest and the berm (Figs. 6a and b)

3.2. Transitions in height

3.2.1. Hydraulic processes

The height transitions on the crest have a major effect on the overtopping load since flow separation at the height transitions leads to high impact forces at the location of reattachment (Figs. 8 and 9). Flow separation occurs in case of a vertical drop similar to the process at the landward crest line shown in previous studies (Ponsioen et al., 2019; Van Bergeijk et al., 2022). In case of a vertical rise, the flow sweeps up and travels through the air before the flow impacts on the surface vertical rise. The impact does not only result in high normal forces and peak pressures, but also high shear stresses because of the large forward motion of the flow in the air after a vertical rise (Fig. 10). This is illustrated by the impact location that is further downstream for a vertical rise (≈1.5 m in Fig. 8) compared to a vertical drop (≈ 0.75 m in Fig. 9). The impact as the result of a vertical rise results in a higher load compared to the load behind a vertical drop: the peaks in the shear stress and the normal stress between x = 6–9 m as the result of the vertical rise at x = 5 m is higher compared to the peak between

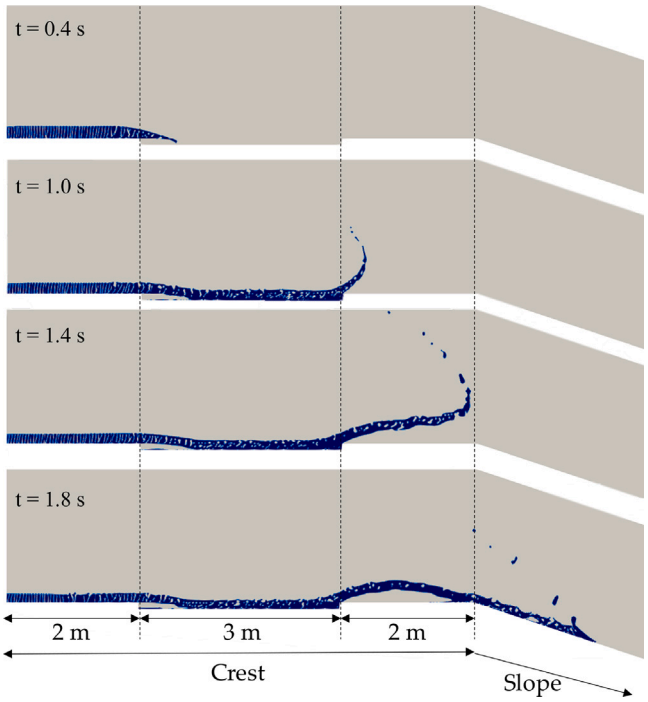

Fig. 9. Screenshots of the overtopping flow at time t for height transitions on the crest with a height of 10 cm below the crest level ($H11$).

x = 2–3 m due to the vertical drop at x = 2 m (see run $H11$ in Fig. 10). This is explained by the flow that reaches a greater height in the air behind a vertical rise and therefore the water impacts from a greater height (Figs. 8 and 9). The numerical model output shows high impact pressures on the vertical rise of the height profile similar to pressures on a vertical wall on the crest (De Finis et al., 2020; Jacobsen et al., 2018).

The location of the maximum load occurs on the crest in case of the height transition located above the crest level (H8 in Fig. 10) compared to the height transition below the crest level where the maximum load is on the upper slope (x > 7 m for H11 in Fig. 10). The maximum load in case of height transitions on the slope occurs in the erosion hole for the majority of the overtopping volumes, but the impact location for larger overtopping volumes and small heights is landward of the hole on the slope. For example, an erosion hole with a depth of 20 cm has a width of 54 cm and a wave with V = 4.0 m^3/m flows completely over this erosion hole with an impact location of more than 54 cm from the transition (Van Bergeijk et al., 2021b).

3.2.2. Comparison to the analytical impact model

The location of impact s_x depends on the height d and can be calculated using the analytical impact model Appendix B. The impact location calculated using the analytical impact model corresponds well to the impact location in the numerical model with a high NSE of 0.80 (Fig. 11c). This means that the analytical impact model can be used to calculate the location of maximum load for height transitions on the crest and the slope where failure of the cover is expected. The analytical model only calculates the impact location due to a vertical drop and cannot be used to calculate the impact location due to a vertical rise (Section 5.2).

3.2.3. Relations for the shear and normal stress

The height transitions significantly affect the shear stress and the normal stress (Fig. 11). Especially the height transitions on the crest have a large effect leading to an increase up to a factor 5 for the shear stress and up to a factor 10 for the normal stress (Fig. 11a).

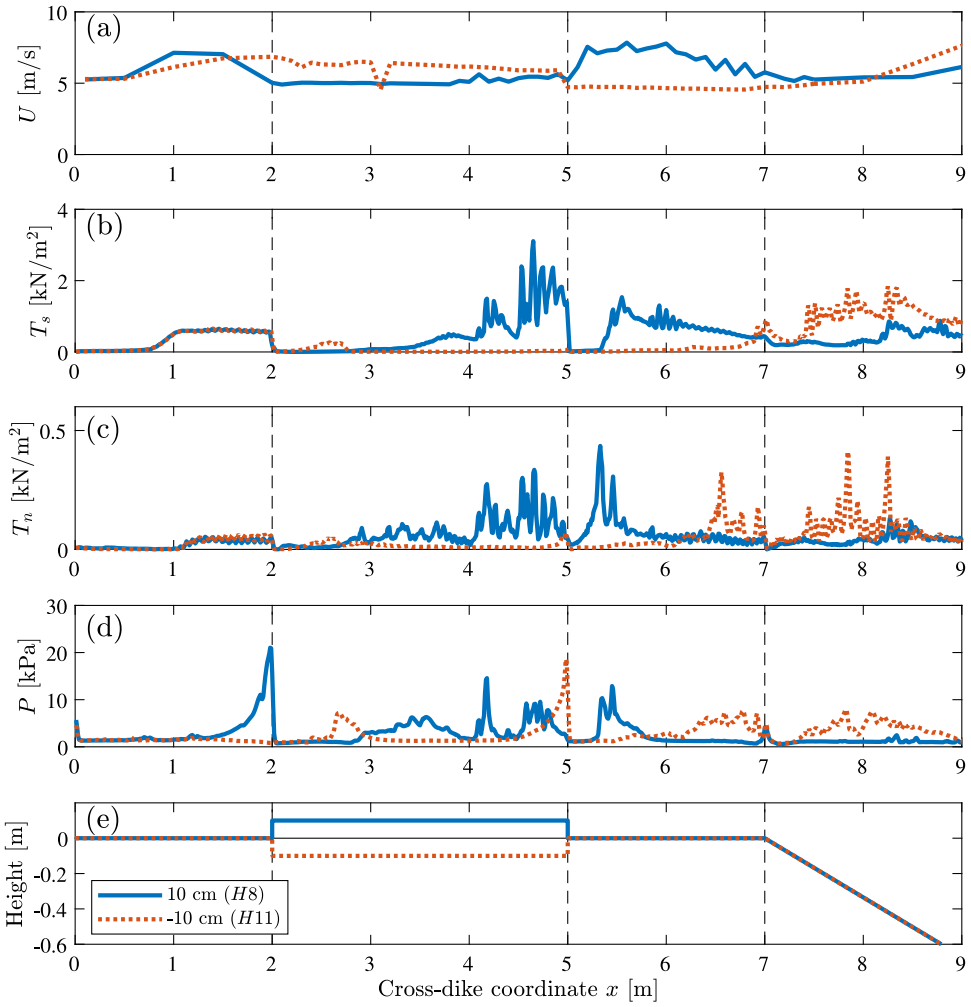

Fig. 10. The hydraulic variables along the crest and the upper landward slope for height transitions on the crest where the dashed lines indicate the height transitions and the landward crest line. (a) the maximum flow velocity U, (b) the maximum shear stress T_s, (c) the maximum normal stress T_n, (d) the maximum pressure P and (e) the profiles.

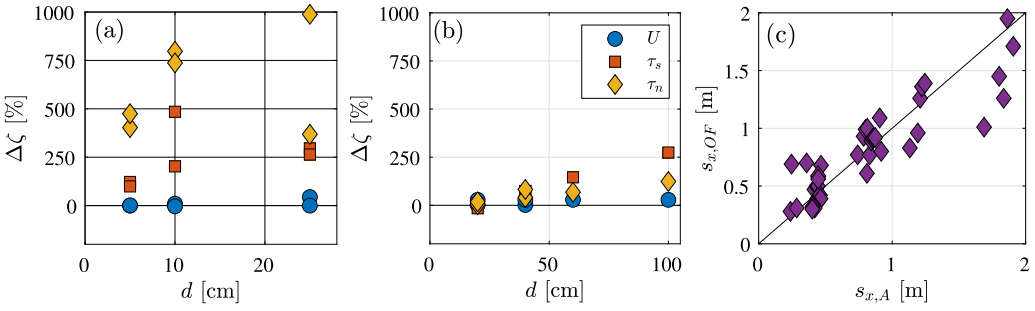

Fig. 11. (a) The effect of height transitions on the crest with height d compared to the reference case without transitions for $V = 2.0$ m^3/m. (b) The effect of height transitions on the slope with height d compared to the reference case without transitions for $V = 2.0$ m^3/m. (c) Comparison of the modelled location of impact at a height transition using the OpenFOAM model $s_{x,OF}$ and the analytical model $s_{x,A}$ with a NSE of 0.80.

A relation for the maximum shear stress T_s and the maximum normal stress T_n as function of the maximum flow velocity U and the height d was derived for height transitions on the crest and the slope based on a regression analysis (Fig. 12). The relation for the maximum load as the result of height transitions on the crest is given by

$$T_{s,crest} = \max(72.1\, d^{1/5}U^2 - 196, 0) \quad \text{for } d = 0.05\text{–}0.25 \text{ m} \tag{6}$$

$$T_{n,crest} = \max(12.0\, d^{1/6}U^2 + 24, 0) \quad \text{for } d = 0.05\text{–}0.25 \text{ m} \tag{7}$$

The shear stress and the normal stress have the dimensions N/m^2 and therefore the coefficients of the fits have the dimensions 72.1 kg/m$^{16/5}$, 196 N/m^2, 12.0 kg/m$^{19/6}$ and 24 N/m^2. The maximum load for height transitions on the slope shows a higher dependency on the height of the transition

$$T_{s,slope} = \max(29.4 d^{1/3}U^2 - 443, 0) \quad \text{for } d = 0.2\text{–}1.0 \text{ m} \tag{8}$$

$$T_{n,slope} = \max(11.8 d^{1/3}U^2 - 108, 0) \quad \text{for } d = 0.2\text{–}1.0 \text{ m} \tag{9}$$

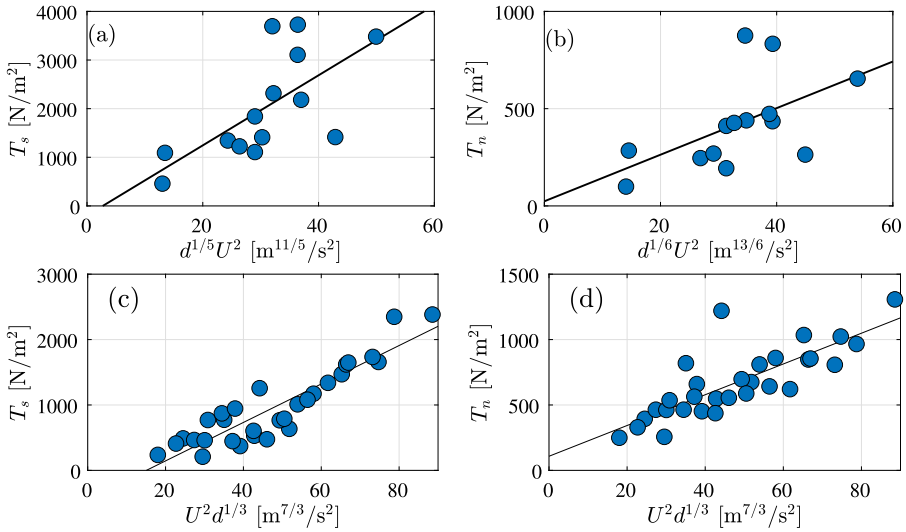

Fig. 12. The modelled maximum load as result of a height transitions as function of the flow velocity U and height d together with a fit through the model results. (a) The maximum shear stress T_s for a height transition on the crest with the best fit $T_s = 72.1d^{1/5}U^2 - 196$ with a NSE of 0.45, (b) The maximum normal stress T_n for a height transition on the crest with the best fit $T_n = 12.0d^{1/6}U^2 - 24$ with a NSE of 0.30. (c) The maximum shear stress T_s for a height transition on the slope with the best fit $T_s = 0.029d^{1/3}U^2 - 0.44$ with a NSE of 0.82. (d) The maximum normal stress T_n for a height transition on the slope with the best fit $T_n = 0.012d^{1/3}U^2 + 0.11$ with a NSE of 0.60.

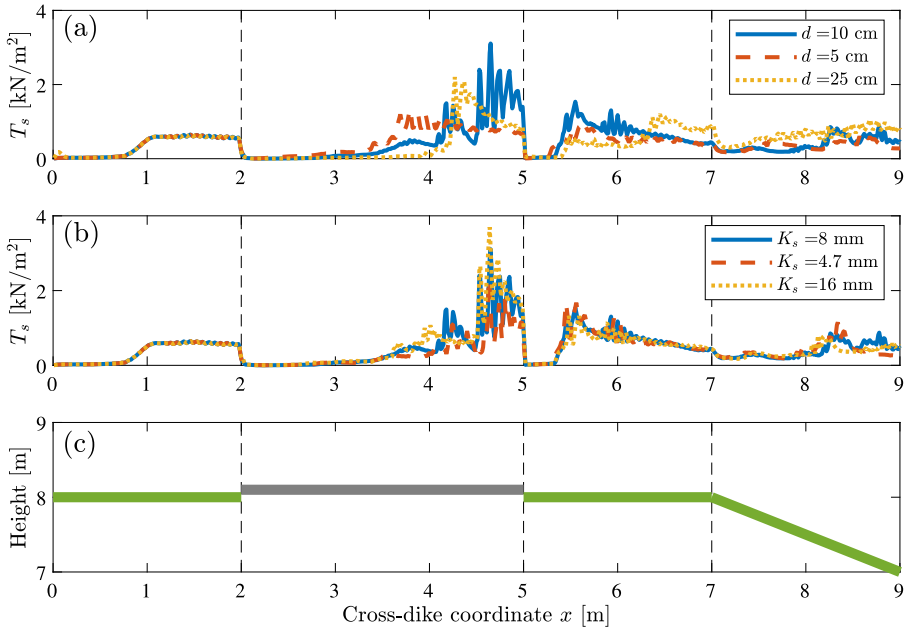

Fig. 13. The maximum shear stress T_s for a transitions in cover type and height on the crest. The reference case (blue) with a height of $d = 10$ cm and a grass cover ($K_s = 8$ mm) is compared to (a) transitions with a grass cover and different heights d, and (b) transitions with a height of 10 cm and different cover types simulated with the roughness height K_s. (c) The dike profile with the transition in height and cover type at $x = 2$ m and $x = 5$ m.

where the coefficients have the dimensions 29.4 kg/m$^{10/3}$, 443 N/m^2, 11.8 kg/m$^{10/3}$ and 108 N/m^2.

The height has a smaller effect on the shear stress and normal stress for height transitions on the crest compared to height transitions on the slope. A possible explanation is that the height transition on the slope only consists of a vertical drop while the transition on the crest also include a vertical rise. The impact forces as the result of a vertical rise dominate over the impact forces as the result of the vertical drop on the crest (Fig. 10). The model results suggest that the height of the vertical rise only has a minor influence on the impact forces.

3.3. Combination of transitions in cover type and height

Combinations of transitions in cover type and height are modelled on the crest to determine the relative effects of both transitions. Changing the roughness of the cover type has a small effect on the magnitude of the load, but does not affect the location of maximum load as illustrated for the maximum shear stress in Fig. 13b. Changing the height of the transitions has a larger effect on the magnitude of the shear stress as well as the location of maximum shear stress (Fig. 13a). This shows that transitions in height have a large influence on the load compared to transitions in cover type. This is further supported by the increase in load calculated for the transitions in cover type (Fig. 6) and

in height (Fig. 11) showing a larger increase in the hydraulic variables for transitions in height.

4. Practical implications for the hydraulic load at transitions

The effect of transitions in cover and in height on the hydraulic load can be summarised as follows:

- *Transition from a smooth to a rough cover*: the flow velocity decreases and the overtopping wave decelerates resulting in a shift of the maximum load along the profile towards the water side and an increase in the overtopping duration.
- *Transition from a rough to a smooth cover*: the flow velocity increases and the overtopping wave accelerates resulting in a shift of the maximum load along the profile towards the landward side and a decrease in the overtopping duration.
- *Height transition with a vertical drop*: the flow separates and results in high impact forces at the location of reattachment.
- *Height transition with a vertical rise*: the flow impacts on the vertical rise leading to high peak pressures. Next, the flow sweeps up into the air and exerts a high hydraulic load at the location of reattachment.

Additionally, the model results showed that combinations of transitions in height and cover type can be treated as transitions in height.

Now, we will use the model results to derive formulations for the load at transitions that can be used in two existing erosion models: the COM (Van Der Meer et al., 2010) and the GEM (Van Bergeijk et al., 2021a). Transitions in cover type have a limited effect on the hydraulic load with an increase of less than 20%. This maximum increase in load of 20% translates to a maximum load factor α_M of 1.2 in the COM (Table 3), which is lower than the theoretically derived load factor but within the calibrated range (Table B.6). This lower load factor for the transition in cover type agrees with the calibrated load factor of 1.1–1.2 for the transition from asphalt to grass based on the majority of the overtopping experiments (Van Der Meer et al., 2015). The analytical model for the maximum flow velocity is used to calculate the load in the GEM and this model is able to accurately calculate the effect of transitions in cover type for larger overtopping volumes ($V = 2.0$ m^3/m). Another way to simulate the increase in load at transitions is by using the turbulence parameter ω in the GEM. The turbulence parameter for transitions in cover type based on the model results varies between 2.3–2.9, which is based on an increase of 20% for the theoretical and the measured turbulence parameter on the slope and crest (Tables 3 and B.6).

For transitions in height, the flow separates at the height transition and the maximum load occurs at the impact location where the flow reattaches to the dike cover. The analytical impact model works well to predict the impact location as the result of height transitions with a vertical drop. The hydraulic load as the result of height transitions was quantified using the numerical model and the results were used to derive relations for the maximum normal stress and the maximum shear stress as function of the height and the flow velocity (Eqs. (6)–(9)). The gradient of these fits in Fig. 12 can be used as a multiplication factor for the flow velocity such as the load factor in the COM and the turbulence parameter in the GEM. For example, the relation for the normal stress in N/m^2 on the slope (Eq. (9)) can be transferred to

$$T_{n,slope} \propto 11.8\, d^{1/3} U^2 = \alpha_M U^2 = \omega^2 U^2 \tag{10}$$

providing a relation for the load factor α_M in the COM and the turbulence parameter ω in the GEM as function of the height d and the constant 11.8. For a height of 0.2 m, this relation results in $\omega = \sqrt{11.8 \cdot 0.2^{1/3}} = 2.6$ (Table 3), which is close to the calibrated turbulence parameter for damages with a maximum height of 0.2 m ($\omega = 2.26$–2.56, Table B.6).

Using the relations for the normal stress and the shear stress to derive a load factor α_M results in high load values that are above the theoretical limit of 2 (Van Hoven et al., 2013) (Table 3). The theoretical relations for the load factor were derived under the assumption of uniform flow conditions, while turbulence is the main driver of the erosion process at transitions and could be a reason for the high load factors. Another possible explanation is that the COM only describes erosion as the result of scour erosion and not by impact forces that are the cause of the high hydraulic load at height transitions. Additionally, the erosion threshold U_c in the erosion models should be adapted to a threshold for normal loading in N/m^2. For example, Hoffmans (2012) suggests a critical normal stress between 50–125 N/m^2 for an average grass quality that could be used as an erosion threshold in the erosion models, but this value should be validated.

Table 3
Multiplication factors for the load at height transitions and transitions in cover type based on the model results and the gradients of the fits for the shear stress T_s and the normal stress T_n (Eqs. (6)–(9)).

	Height				Cover
	$T_{s,crest}$	$T_{n,crest}$	$T_{s,slope}$	$T_{n,slope}$	$\Delta\zeta_{cover}$
Load factor α_M	52.3	9.2	17.2	6.9	1.2
Turbulence parameter ω	7.2	3.0	4.2	2.6	2.3 – 2.9

5. Discussion

5.1. The load at transitions in cover type and in height

Transitions in the field are often a combination of transitions in cover type and in height, for example an asphalt road that is located higher than the surrounding grass cover. The numerical model results show that the relative effect of transitions in cover type on the load is less than 20% of the reference case (Fig. 6), while height transitions on the crest and the slope result in more than doubling of the reference load up to 800% (Fig. 11). These results are in agreement with the case study of an asphalt road on top of a dike by Bomers et al. (2018) who found a similar increase in magnitude for the transition from the asphalt cover to grass and geometric effects, such as the height differences between the cover and the road. In this study, the relative effects of transitions in cover type and transitions in height were systematically investigated and we conclude that transitions in height dominate over transitions in cover type. Therefore, realistically occurring transitions in both cover type and height can be treated as a transition in height.

Additionally, new descriptions of the hydraulic load including the effects of transitions in cover type and height were derived in this study (Fig. 14). Transitions in cover type mainly affect the flow velocity and the analytical formulas of Van Bergeijk et al. (2019b) can be used to predict the magnitude of the flow velocity and the location of maximum flow velocity. These formulas have previously been validated for a wide range of overtopping volumes and dike configurations. In this study, the analytical formulas were validated for transitions in cover type with a Nikuradse roughness height varying between 1 mm and 16 mm on the crest and a landward berm.

Transitions in height result in flow separation and high impact forces at the location of reattachment. The magnitude of the hydraulic load as the result of a height transitions can be calculated using the newly developed relations for the maximum shear stress and the maximum normal stress. The relations for height transitions on the crest describe the maximum load as result of a vertical drop and a vertical rise and were validated for heights of 5–25 cm and overtopping volumes of 0.6–3 m^3/m. The relations for height transitions on the slope only describe the maximum load due to a vertical drop and were validated for heights of 20–100 cm and overtopping volumes of 1–4 m^3/m. The location of maximum load due to a vertical drop is calculated using the analytical impact model described in Appendix B.2.

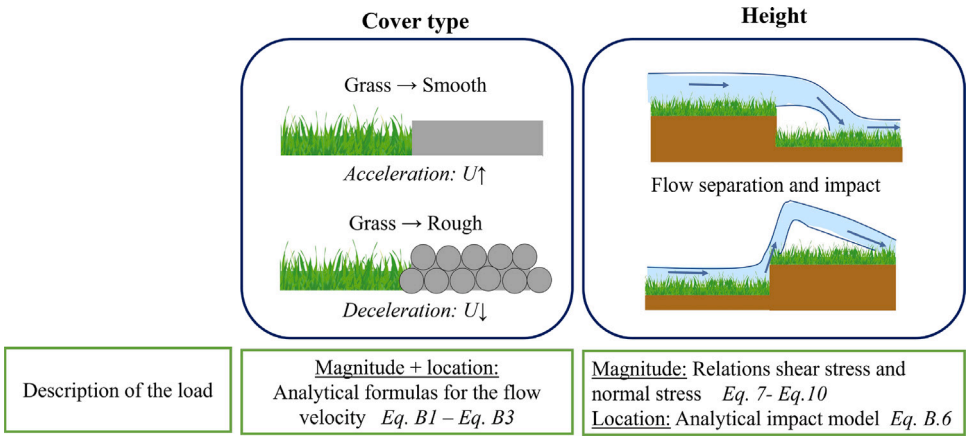

Fig. 14. Summarising figure of the effects of transitions in cover type and in height on the hydraulic load and the developed methods.

Table 4
The ratio between the height of the transition (wall) d and the layer thickness on the crest h_{crest} determines the amount of overtopping reaching the landward side of the flood defence.

Condition	Example	Overtopping over the wall
$d \gg h_{crest}$	Buildings	No overtopping
$d > h_{crest}$	Storm wall, crest wall, crown wall	Limited overtopping
$d < h_{crest}$	Roads, damages	Overtopping

The analytical impact model is validated using both the height transitions on the crest and the slope with a validation range of d =5–100 cm and V = 0.6–4 m^3/m.

The numerical model uses the maximum flow velocity and the maximum layer thickness as function of time as model input based on the overtopping volume (Eq. (1). A similar method can be used to calculate the maximum flow velocity required for the analytical models and the relations for the shear stress and normal stress (Eq. (B.4).

5.2. Impact forces at height transitions

The overtopping flow against the vertical rise of a height transition on the crest shows similarities with the overtopping flow against vertical walls and buildings on the crest. The vertical rise experiences high impact forces as seen in the modelled pressure (Fig. 10d) similar to the impact forces and pressures measured during experiments (Chen et al., 2015, 2016; Van Doorslaer et al., 2017) and observed in numerical models (Jacobsen et al., 2018; De Finis et al., 2020; Molines et al., 2020). Similar to the derived relations for the shear stress and the normal stress, Van Doorslaer et al. (2017) showed that the force proportional to the quadratic relationship between U and the kinetic energy (USACE, 1984). Van Doorslaer et al. (2017) also investigated the dependency of the impact force on the layer thickness h where the best prediction shows that the force is proportional to $(Uh)^{1/3}$. Further investigation of the relation between impact force and the layer thickness is recommended, especially since the ratio between the layer thickness and the height of the transition affects the amount of overtopping flow reaching the landward slope (Table 4). In case the height of the transition d is much larger than the layer thickness on the crest h_{crest}, no water will overtop the structure as is the case for buildings on the crest (Chen et al., 2015, 2016). Limited overtopping will occur in case the height of the transition is higher than the layer thickness (Van Doorslaer et al., 2017; Jacobsen et al., 2018; De Finis et al., 2020; Molines et al., 2020). The height transitions with a vertical rise studied in this paper have a height smaller than the layer thickness and therefore do not (noticeable) limit the amount of overtopping flow reaching the landward slope.

Previous studies on the impact forces of vertical walls have focused on the structural response and stability under wave overtopping. However, the vertical wall in case of a height transitions on the crest can be an erodible cover, for example when the grass cover is located higher compared to an asphalt road. Vertical rises are sensitive for erosion due to the high impact forces. Therefore, the design of transitions could be improved so height transitions are avoided or followed by a non-erodible material such as asphalt. Examples are the use of grass concrete blocks, Elastocoast or geogrid to reduce the difference in height or improve the strength of the grass cover at the expected impact location (Van Steeg and van Hoven, 2013; Scheres and Schüttrumpf, 2020). Height differences often occur at transitions in cover type as the result of maintenance issues such as problems with mowing and grazing (Van Steeg and van Hoven, 2013). Therefore, designing transitions in such a manner that they are better and easier to maintain is also a possibility to reduce the number of height transitions.

For transitions in height, the flow separates at the height transitions and the maximum load occurs at the impact location where the flow reattaches to the dike cover. This process is similar to the flow separation at the landward crest line and impact on the upper slope observed during wave overtopping experiments and in numerical models (Van Damme et al., 2016; Ponsioen et al., 2019; Van Bergeijk et al., 2022). The analytical impact model works well to predict the impact location as the result of a height transitions with a vertical drop. The impact locations predicted with the analytical impact model were compared to the numerical model results and could be further validated using overtopping field tests (Van Bergeijk et al., 2021b). The impact location is calculated as a point in the analytical impact model since it is based on the trajectory of a projectile. In reality, the flow spreads and thereby the location of impact is actually an area of impact. The analytical impact model can be extended to describe an impact area similar to the approach of Ponsioen et al. (2019) that describes the impact area for flow separation at the landward crest line. Furthermore, the analytical impact model could be extended to calculate the impact location behind a height transition with a vertical rise. This is especially important for transitions on the crest where the numerical model results show that the impact forces due to the vertical rise are larger than the impact forces due to the vertical drop.

Moreover, it is recommended to study more gradual height transitions with slopes. In this study, only height transition with a 90 ° rise or drop were studied, which is the most extreme case of geometric transitions. For more gradual height transitions with a slope, the location of reattachment could depend on the slope angle of the profile before separation and the slope angle of the profile at the reattachment, similar to the third-order polynomial found by Paarlberg et al. (2007) for flow separation over river dunes.

5.3. Model limitations

This study was limited to 2DV transitions that are uniform in the along-dike direction since the OpenFOAM® model is a 2DV model. An extension of the OpenFOAM® model to the third dimension makes it possible to study the effect of 3D transitions on the load such as trees, stairs and houses on flood defences. For example, Chen et al. (2021c) simulated the overtopping forces on a human body on the crest using a 3D OpenFOAM® model. However, measurements of the 3D overtopping flow on the landward slope are necessary to validate a 3D model before the model could be extended. These types of measurements are currently not available and are recommended to perform in future overtopping experiments.

The numerical model simulations are performed with an impermeable surface with the assumption of no infiltration of water in the cover and the core material. The amount of infiltration depends on the permeability of the soil (Hoffmans, 2012) and might have an effect on the hydraulic load. This study is therefore only representative for a grass cover on an impermeable clay layer. For future studies, the permeability of cover material can be included in the numerical model using a porosity layer as shown in simulations of the overtopping flow over flood defences with block revetments (Chen et al., 2021a; Barendse et al., 2022; Jacobsen et al., 2015).

The different cover types are simulated using a Nikuradse roughness height K_s in the numerical model and the friction factor f in the analytical model. The Nikuradse roughness height in the model accounts both for the roughness of the cover type as well as small geometric variations within a grid cell that are solved using the roughness height in the numerical model. A uniform roughness is assumed for each cover type while the roughness of the cover may vary over time and along the profile. For example, the bed roughness changes as the cover erodes due to a change in cover type, e.g. from grass to clay, as well as the erosion pattern that increases the irregularities of the cover and thereby the roughness (Van Bergeijk et al., 2020; Bomers et al., 2018). Geometric irregularities smaller than the grid size can be simulated in the numerical model using the Nikuradse roughness height (Van Bergeijk et al., 2020), however, larger irregularities need to be included in the grid itself. The simulations of the height transitions are a first step to determine how geometric irregularities affect the overtopping wave. Further investigation into the relation between geometric irregularities and cover roughness, and how to incorporate these effects in analytical and numerical models is recommended.

The formation of a water layer in front of a height transitions with a vertical rise was observed during experiments that can lead to energy dissipation and damping of the wave forces (Hoffmans and Verheij, 2011; Bakker et al., 2013). This was not included in the numerical model simulations, since only one overtopping wave is simulated and therefore no water of the previous overtopping wave is present. An additional model run was performed with a water layer of 5 cm in front of the height transition to study the effect of water collection in front of a height transition on the hydraulic load (Fig. 15). The overtopping wave impacts on the water layer in front of the height transition instead of the height transition. Therefore, the flow reattaches to the dike surface at a cross-dike location of $x \approx 3$ m instead of $x \approx 4.5$ m. The magnitude of the maximum normal stress is similar for both cases, but the location of the maximum normal stress changes. The maximum occurs on the elevated surface (e.g. the road) for the simulation with a water layer while the normal stress is maximum behind the vertical drop for the simulation without a water layer. The water layer reduces the pressure on the vertical rise at $x = 2$ m but leads to higher pressures in front of the vertical rise ($x = 0$–2 m). Overall, water collection in front of a height transition does not affect the maximum load but affects the location where the maximum occurs.

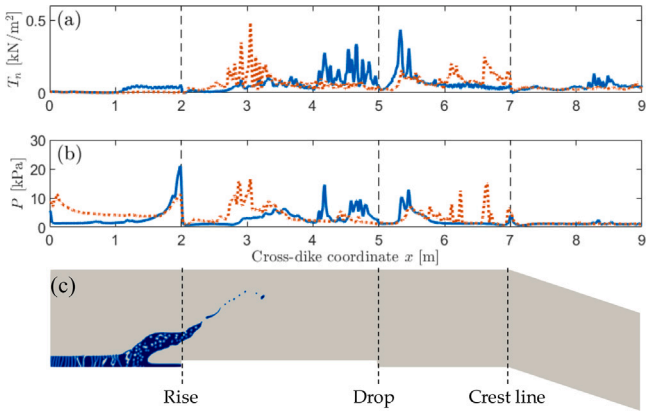

Fig. 15. Comparison of the hydraulic load for a transition in height on the crest without a water layer (blue solid) and with a water layer (orange dashed) in front of the vertical rise. (a) The maximum normal stress T_n. (b) The maximum pressure P. (c) Snapshot of the simulation with a water layer at $t = 0.45$ s.

5.4. Including the effects of transitions in erosion models

The main implication of this study is that the quantification of the load can help to include the effects of transitions on the hydraulic load in wave overtopping erosion models (Fig. 14). The gained insights into the effects of transitions on the hydraulic load can be used to predict the cover erosion by overtopping waves for flood defences with various transitions. Van Bergeijk et al. (2022) showed how the effect of slope changes on the hydraulic load can be included in erosion models based on different hydraulic variables. The same approach can be applied to transitions in height and in cover type using the new relations for the shear stress and the normal stress or using the multiplication factors derived in Section 4.

For transitions in cover type, a multiplication factor for the load of 1.2 is recommended based on the maximum increase in load. Another way to describe the effect of transitions in cover type is to use the analytical model for the flow velocity Appendix B.1 (Van Bergeijk et al., 2019b) that showed good agreement with the numerical model results, although the effect on the flow velocity is underestimated for small overtopping volumes. Although transitions in cover type have a limited effect on the magnitude of the load, the overtopping duration increases for rough covers and decreases for smooth covers (Bomers et al., 2018; Van Bergeijk et al., 2020). The overtopping duration is included in the GEM and the erosion models of Dean et al. (2010) and Hoffmans (2012). In these erosion models, a rough cover could lead to more erosion due to a larger overtopping duration compared to a smooth cover. This is also the case for erosion models that integrate the load over the overtopping duration such as the model of Ponsioen et al. (2019) and Aguilar-López et al. (2018). However, Van Bergeijk et al. (2022) found that the integration of the overtopping load over the duration does not provide additional information and is therefore not recommended to limit complexity.

Transitions in height influence both the maximum load and the location of the maximum load. The analytical impact model can predict the location of maximum hydraulic load using the height of the transition and the flow velocity, which depends on the overtopping volume and the cover type. The load as result of transitions in height can be included in existing calculation methods using a multiplication factor for the flow velocity. The obtained relation for the maximum shear stress and maximum normal stress at height transitions can be used to determine these multiplication factors (Table 3). The fits express the load in N/m^2, that should be either transferred to m^2/s^2 in the COM or GEM, or the damage number in the COM or the erosion threshold and erosion rate in the GEM should be adapted so the load in N/m^2 can be included.

The numerical model results show that it is important to include the effect of upstream transitions on the downstream flow. The transitions in cover type on the crest affect the location of maximum shear stress on the slope (Fig. 7) and the height transitions on the crest result in high hydraulic loads on the upper landward slope (Fig. 10). The COM is only applied to the weakest location along the profile and therefore the effect of upstream transitions on the load are not included. The downstream effects of transitions on the flow velocity are included in the GEM using the analytical flow velocity model. However, the turbulence parameter is only locally adapted for transitions and does not include the effect of upstream transitions on the turbulence parameter. Further development of the analytical model for height transitions or another method to include the effect of upstream transitions in the COM and the GEM is recommended for future research.

6. Conclusions

The aim of this study was to quantify the effects of transitions in cover type and in height on the overtopping load and determine the important hydraulic processes at these transitions. Numerical simulations were performed to determine the flow velocity, the shear stress, the normal stress and the pressure along the crest and the landward slope. The results show that transitions lead to more than doubling of the overtopping load compared to the situation without a transition. We observed a relatively small effect of transitions in cover type on the hydraulic load with a maximum increase of around 20%. Therefore, transitions in height dominate over transitions in cover type, which means that combinations of transitions in cover type and height can be treated as a transition in height only.

The increase in the load as the result of transitions was translated to the load predicted by three existing methods: (1) the analytical model for the flow velocity, (2) the load factor in the COM, and (3) the turbulence parameter in the GEM. The transition from a rough to a smooth cover results in an acceleration of the flow and the flow decelerates for a transition from a smooth to a rough cover. These effects on the flow velocity were accurately simulated using the analytical model. In other models, a multiplication factor of 1.2 for the load can be used to account for the effect of transitions in cover type on the hydraulic load.

Transitions in height result in flow separation and high hydraulic loads at the impact location. The formulas for the trajectory of a projectile were used to calculate this impact location using the height of the transitions and the flow velocity of the overtopping wave. The impact location is an important variable since this is the location where the load is maximal and erosion of the grass cover is most likely to start. Relations for the maximum shear stress and the maximum normal stress as the result of transitions in height were derived from the model results to calculate the increase in load at these transitions. The relations are a function of the height of the transition and can be used in existing erosion models based on the shear stress and the normal stress.

Additionally, the results showed that transitions affect the downstream hydraulic load, and therefore it is important to include the effect of upstream transitions on the hydraulic load at landward slopes. The downstream effect of transitions in cover type on the maximum flow velocity are included in the analytical formulas of Van Bergeijk et al. (2019b), but the load description in erosion models need to be adapted so the effect of height transitions on the downstream load can be included.

Transitions are vulnerable locations for cover erosion by overtopping waves and therefore it is crucial to include the effects of transitions in the design and the safety assessment of flood defences. This model study quantified the hydraulic load as the result of transitions. Further research into the cover strength at transitions is required to predict the erosion near transitions. Additionally, limited measurements at transitions are available although these measurements provide valuable information on the flow at transitions. Therefore, measurements at transitions such as roads, slope changes and damages are advised to increase our understanding of the effects of transitions on the overtopping flow. Geometric transitions have a major influence on the overtopping load and therefore these transitions are extremely important to consider in the design of flood defences. Improvements to the design of such transitions are recommended to investigate, for example more gradual slope and height changes, to increase the safety of flood defences.

CRediT authorship contribution statement

Vera M. van Bergeijk: Conceptualization, Methodology, Software, Validation, Writing – original draft, Writing – review & editing, Visualization. **Jord J. Warmink:** Conceptualization, Writing – review & editing, Supervision, Project administration, Funding acquisition. **Suzanne J.M.H. Hulscher:** Conceptualization, Writing – review & editing, Supervision, Project administration, Funding acquisition.

Declaration of competing interest

The authors declare the following financial interests/personal relationships which may be considered as potential competing interests: Vera van Bergeijk reports financial support was provided by Netherlands Organisation for Applied Scientific Research. Vera van Bergeijk reports financial support was provided by Rijkswaterstaat Water Traffic and Living Environment. Vera van Bergeijk reports financial support was provided by European Regional Development Fund.

Acknowledgements

This work is part of the research programme All-Risk, Implementation of new risk standards in the Dutch flood protection program (P15-21), which is (partly) financed by the Netherlands Organisation for Scientific Research (NWO). Additionally, this work was funded by Rijkswaterstaat and funded by the Interreg 2 Seas program 2014–2020, co-funded by the European Regional Development Fund with contract number 2S07-023. This work was carried out on the Dutch national e-infrastructure with the support of SURF Cooperative. Finally, we want to thank the reviewers for their constructive comments that greatly improved the quality of this paper.

Appendix A. Overview of the model runs

See Table A.5.

Appendix B. Analytical models and multiplication factors for transitions

B.1. Analytical model for the flow velocity

Van Bergeijk et al. (2019b) developed an analytical model for the wave overtopping flow velocity along the crest and the landward slope consisting of two formulas: one for horizontal parts, such as the crest and a berm, and one for slopes:

$$U_{a,horizontal}(x) = \left(\frac{fx}{2Q} + \frac{1}{U_{a,horizontal}(x=0)} \right)^{-1} \tag{B.1}$$

$$U_{a,slope}(x) = \frac{\alpha}{\beta} + \mu \exp\left(\frac{-3\alpha\beta^2 x}{\cos\varphi} \right) \tag{B.2}$$

where x is the cross-dike coordinate, Q is the momentary discharge, φ is the slope angle and the factors α, β and μ are given by

$$\alpha = \sqrt[3]{g \sin\varphi},\ \beta = \sqrt[3]{f/2Q},\ \text{and}\ \mu = U_{a,slope}(x=0) - \frac{\alpha}{\beta}. \tag{B.3}$$

These formulas are coupled through the flow velocity at the start of the profile part $U_a(x = 0)$ and can be used to calculate the flow velocity along the profile for flood defences with different cover types and

Table A.5
Overview of the model runs of transitions in cover type ($C1$–$C10$), transitions in height ($H1$–$H12$) and combinations of both ($CH1$–$CH4$) including the cross-dike location, the roughness height K_s, the height d and the simulated overtopping volumes V.

Runs	Location	K_s [mm]	d [cm]	V [m^3/m]
$C1$	Crest (x = 2–5 m)	8	–	0.6, 2
$C2$	Crest (x = 2–5 m)	1	–	0.6, 2
$C3$	Crest (x = 2–5 m)	4.7	–	0.6, 2
$C4$	Crest (x = 2–5 m)	10	–	0.6, 2
$C5$	Crest (x = 2–5 m)	16	–	0.6, 2
$C6$	Berm (x = 12–15 m)	8	–	2
$C7$	Berm (x = 12–15 m)	1	–	2
$C8$	Berm (x = 12–15 m)	4.7	–	2
$C9$	Berm (x = 12–15 m)	10	–	2
$C10$	Berm (x = 12–15 m)	16	–	2
$H1$	Upper slope (x = 10 m)	8	20	1, 2, 2.5, 3, 4
$H2$	Upper slope (x = 10 m)	8	40	1, 2, 2.5, 3, 4
$H3$	Middle slope (x = 17 m)	8	20	1, 2, 2.5, 3, 4
$H4$	Middle slope (x = 17 m)	8	40	1, 2, 2.5, 3, 4
$H5$	Middle slope (x = 17 m)	8	60	1, 2, 2.5, 3, 4
$H6$	Middle slope (x = 17 m)	8	100	1, 2, 2.5, 3, 4
$H7$	Crest (x = 2–5 m)	8	5	2
$H8$	Crest (x = 2–5 m)	8	10	0.6, 2, 3
$H9$	Crest (x = 2–5 m)	8	25	2
$H10$	Crest (x = 2–5 m)	8	−5	2
$H11$	Crest (x = 2–5 m)	8	−10	0.6, 2, 3
$H12$	Crest (x = 2–5 m)	8	−25	2
$CH1$	Crest (x = 2–5 m)	4.7	10	2
$CH2$	Crest (x = 2–5 m)	16	10	2
$CH3$	Crest (x = 2–5 m)	4.7	−10	2
$CH4$	Crest (x = 2–5 m)	16	−10	2

geometries. The effects of transitions are included by locally adapting the slope angle φ or the friction factor f.

The analytical model requires the flow velocity on the crest u_0 and the momentary discharge Q as boundary conditions. These can be computed using empirical relations (Van Der Meer et al., 2010; Hughes and Shaw, 2011) and the overtopping volume V

$$u_0 = 4.5\,V^{0.34}, \quad h_0 = 0.133\,V^{0.5} \quad \text{and} \quad Q = h_0\,u_0 = 0.6\,V^{0.84}. \tag{B.4}$$

B.2. Analytical impact model

Geometric transitions lead to flow separation where the flow reattaches to the cover at the impact location s_x (Fig. 4). The analytical impact model calculates the impact location using the basic formulas for the trajectory of a projectile. Firstly, the vertical trajectory is set to the height d and solved for the time t

$$U\sin(\varphi)t + \frac{1}{2}gt^2 = d \quad \rightarrow \quad t = \frac{U\sin(\varphi) + \sqrt{2\,gd + U^2\sin(\varphi)^2}}{g} \tag{B.5}$$

Next, the time t is used to calculate the impact location using the formula for the horizontal trajectory:

$$s_x = U\cos(\varphi)t \tag{B.6}$$

B.3. Load factor in the COM

The Cumulative Overload Method calculates the damage number D to approximate the amount of erosion (Van Hoven et al., 2013)

$$D = \sum \alpha_a \alpha_M U_0^2 - \alpha_s U_c^2 \tag{B.7}$$

The load is described by the flow velocity on the crest U_0, the acceleration factor α_a for the acceleration on the slope and the load factor α_M for the effect of transitions on the hydraulic load. The strength of the cover is described by the critical flow velocity U_c and the strength factor α_s

Theoretical relations were derived for the load factor at transitions in cover type (Van Hoven et al., 2013). The load increases from a smooth to rough bed ($\alpha_{M,s\rightarrow r}$), while the opposite occurs for the transition from a rough to a smooth bed ($\alpha_{M,r\rightarrow s}$):

$$\alpha_{M,r\rightarrow s} = \left(\frac{n_s}{n_r}\right)^6 \left(\frac{\ln 10h/(8\sqrt{g}\,n_s)^6}{\ln 10h/(8\sqrt{g}\,n_r)^6}\right)^2 \tag{B.8}$$

$$\alpha_{M,s\rightarrow r} = 2 - \alpha_{M,r\rightarrow s} \tag{B.9}$$

with the Manning's coefficient of the smooth n_s and rough n_r cover and the layer thickness h. For the transition from asphalt (n = 0.016) to grass (n = 0.025), the load factor varies between 1.7 and 1.8 depending on the layer thickness (0.1 m–0.5 m). This theoretical load factor agrees with the calibrated value of the test at Millingen a/d Rijn (α_M = 1.8) but is much higher compared to the calibrated values of the other experiments with a transition from grass to asphalt (α_M = 1.1–1.2, Table B.6).

Theoretical formulas describe the effect of slope changes on the load depending on the difference in slope angle θ (Van Hoven et al., 2013). The load increases for a concave slope change, for example the landward toe, due to an increase in the normal forces because the centripetal forces is downward directed.

$$\alpha_M = 1 + \left(\sin\frac{1}{2}\theta\right) \tag{B.10}$$

This results in a load factor of 1.1 and 1.3 for slopes with a steepness of 1:3 and 1:2. Calibration of the load factor at the landward toe based on the overtopping field tests showed higher load factors of 1.3–1.6 for a slope of 1:3 and 1.5–1.8 for a slope of 1:2 (Warmink et al., 2020).

For convex slope changes such as the transitions from the crest to the landward slope, the load decreases according to Van Hoven et al. (2013) as the result of a lower normal force as the centripetal force is directed upwards

$$\alpha_M = 1 - \left(\sin\frac{1}{2}\theta\right) \tag{B.11}$$

The decrease in load for convex slope changes is contrary to the increase in load as the result of flow separation and impact observed by Van Damme et al. (2016) and described by the formulas of Ponsioen et al. (2019) and Van Bergeijk et al. (2022).

B.4. Turbulence parameter in the GEM

The erosion depth z_e is calculated in the analytical Grass-Erosion Model (Van Bergeijk et al., 2021a) as

$$z_e(x) = \sum \left(\omega^2(x)U^2(x) - U_t^2\right) T_0 C_E \tag{B.12}$$

The load depends on the turbulence parameter ω and the maximum flow velocity $U(x)$ along the profile. The strength of the cover is describe by the erosion threshold U_t and the amount of erosion is calculated using the overtopping period T_0 and the inverse cover strength parameter C_E.

The analytical formulas for the flow velocity (Eq. (B.2)) already account for transitions in cover type and slope angle. The turbulence parameter is related to the depth-averaged turbulence intensity r_0 as

$$\omega = 1.5 + 5r_0 \tag{B.13}$$

based on the increase in load as the result of jet impact in scour theory (Jorissen and Vrijling, 1989; Hoffmans, 2012). Hoffmans (2012) reports two formulas for the turbulence intensity that can be applied to horizontal parts of the profile or slopes (Van Bergeijk et al., 2019a)

$$r_0 = 0.85\sqrt{f} \quad \text{for horizontal parts} \tag{B.14}$$

$$r_0 = \sqrt{\frac{gQ\sin\varphi}{U_{max}^3}} \quad \text{for slopes} \tag{B.15}$$

with the maximum flow velocity on the slope U_{max}. The formula predicts ω = 1.925 for grass-covered horizontal parts and ω = 2.1–2.4 for

Table B.6
Theoretical,calibrated and measured values of the load factor α_M in the COM and the turbulence parameter ω in the GEM.

		$\alpha_{M,theory}$	$\alpha_{M,calibrated}$	$\omega_{calibrated}$	ω_{theory}	$\omega_{measured}$
Transition	Asphalt-grass	1.7–1.8	1.1–1.8	–	–	–
	Landward toe	1.1–1.3	1.3–1.8	2.75–3.75	–	–
	Height	–	–	2.26–2.56	–	–
Location	Crest	–	–	–	1.925	2.0
	Slope	–	–	–	2.1–2.4	2.35

grass-covered slopes based on calculations of r_0 by Van Bergeijk et al. (2019a) (Table B.6). These values are close to the turbulence parameter based on measurements of the pressure during a field experiment resulting in $\omega = 2.0$ for the crest and $\omega = 2.35$ for a slope of 1:3 (Van Hoven et al., 2013).

The turbulence parameter has been calibrated for the geometric transitions using the field tests with the overtopping simulator (Warmink et al., 2020; Van Bergeijk et al., 2021a). The calibrated load increase at the landward toe results in $\omega = 2.75$ for mild slopes (1:3) and $\omega = 3.75$ for steep slopes (1:2.3) (Warmink et al., 2020). Damages resulting in a vertical cliff can be identified as a height transitions. The turbulence parameter at damages depends on the grass quality, described by the critical velocity U_c, because the grass quality affects the cover roughness and thereby the amount of turbulence (Van Bergeijk et al., 2021a).

$$\omega = 0.074U_c + 2.1 \tag{B.16}$$

The turbulence parameter for damages varies between 2.26 for poor grass quality and 2.56 for a good grass quality. This relation is also applicable to height transitions; however, the relation was calibrated using damages with a maximum height of 20 cm and needs to be validated for larger heights.

References

Aguilar-López, J.P., Warmink, J.J., Bomers, A., Schielen, R.M.J., Hulscher, S.J.M.H., 2018. Failure of grass covered flood defences with roads on top due to wave overtopping: A probabilistic assessment method. J. Mar. Sci. Eng. 6 (3), 1–28. http://dx.doi.org/10.3390/jmse6030074.

Altomare, C., Crespo, A.J.C., Rogers, B.D., Dominguez, J.M., Gironella, X., Gómez-Gesteira, M., 2014. Numerical modelling of armour block sea breakwater with smoothed particle hydrodynamics. Comput. Struct. 130, 34–45. http://dx.doi.org/10.1016/j.compstruc.2013.10.011.

Bakker, J., Melis, R., Mom, R., Bakker, 2013. Factual Report: Overslagproeven Rivierenland (in Dutch). Technical Report Projectnumber: 12i071, Infram, Maarn, The Netherlands.

Bakker, J., Mom, R., Steendam, G., 2008. Factual Report: Golfoverslagproeven Zeeuwse Zeedijken (In Dutch). Technical Report, Infram, Maarn, The Netherlands.

Barendse, L., Van Bergeijk, V.M., Chen, W., Warmink, J.J., Mughal, A., Hill, D., Hulscher, S.J.M.H., 2022. Hydrodynamic modelling of wave overtopping over a block-covered flood defence. J. Mar. Sci. Eng. 10 (1), 89. http://dx.doi.org/10.3390/jmse10010089.

Blöschl, G., Hall, J., Viglione, A., Perdigão, R.A., Parajka, J., Merz, B., Lun, D., Arheimer, B., Aronica, G.T., Bilibashi, A., Boháč, M., Bonacci, O., Borga, M., Čanjevac, I., Castellarin, A., Chirico, G.B., Claps, P., Frolova, N., Ganora, D., Gorbachova, L., Gül, A., Hannaford, J., Harrigan, S., Kireeva, M., Kiss, A., Kjeldsen, T.R., Kohnová, S., Koskela, J.J., Ledvinka, O., Macdonald, N., Mavrova-Guirguinova, M., Mediero, L., Merz, R., Molnar, P., Montanari, A., Murphy, C., Osuch, M., Ovcharuk, V., Radevski, I., Salinas, J.L., Sauquet, E., Šraj, M., Szolgay, J., Volpi, E., Wilson, D., Zaimi, K., Živković, N., 2019. Changing climate both increases and decreases European river floods. Nature 573 (7772), 108–111. http://dx.doi.org/10.1038/s41586-019-1495-6.

Bomers, A., Aguilar-López, J.P., Warmink, J.J., Hulscher, S.J.M.H., 2018. Modelling effects of an asphalt road at a dike crest on dike cover erosion onset during wave overtopping. Nat. Hazards 93 (1), 1–30. http://dx.doi.org/10.1007/s11069-018-3287-y.

Chen, X., Hofland, B., Altomare, C., Suzuki, T., Uijttewaal, W., 2015. Forces on a vertical wall on a dike crest due to overtopping flow. Coast. Eng. 95, 94–104. http://dx.doi.org/10.1016/j.coastaleng.2014.10.002.

Chen, X., Hofland, B., Uijttewaal, W., 2016. Maximum overtopping forces on a dike-mounted wall with a shallow foreshore. Coast. Eng. 116, 89–102. http://dx.doi.org/10.1016/J.COASTALENG.2016.06.004.

Chen, W., Warmink, J.J., Van Gent, M.R.A., Hulscher, S.J.M.H., 2021a. Numerical investigation of the effects of roughness, a berm and oblique waves on wave overtopping processes at dikes. Appl. Ocean Res. 102971. http://dx.doi.org/10.1016/J.APOR.2021.102971.

Chen, W., Warmink, J.J., Van Gent, M.R.A., Hulscher, S.J.M.H., 2021b. Numerical modelling of wave overtopping at dikes using OpenFOAM®. Coast. Eng. 166, http://dx.doi.org/10.1016/j.coastaleng.2021.103890.

Chen, H., Yuan, J., Cao, D., Liu, P.L.F., 2021c. Wave overtopping flow striking a human body on the crest of an impermeable sloped seawall. Part II: Numerical modelling. Coast. Eng. 168, 103892. http://dx.doi.org/10.1016/J.COASTALENG.2021.103892.

Chow, V., 1959. Open-Channel Hydraulics. McGraw-Hill Book Company, Inc. New York, US.

De Finis, S., Romano, A., Bellotti, G., 2020. Numerical and laboratory analysis of post-overtopping wave impacts on a storm wall for a dike-promenade structure. Coast. Eng. 155, 103598. http://dx.doi.org/10.1016/J.COASTALENG.2019.103598.

Dean, R.G., Rosati, J.D., Walton, T.L., Edge, B.L., 2010. Erosional equivalences of levees: Steady and intermittent wave overtopping. Ocean Eng. 37 (1), 104–113. http://dx.doi.org/10.1016/j.oceaneng.2009.07.016.

EurOtop Manual, 2018. In: Van der Meer, J., Allsop, N., Bruce, T., De Rouck, J., Kortenhaus, A., Pullen, T., Schüttrumpf, H., Troch, P., Zanuttigh, B. (Eds.), Manual on Wave Overtopping of Sea Defences and Related Structures. an Overtopping Manual Largely Based on European Research, but for Worldwide Application. Technical Report, URL: www.overtopping-manual.com.

Heida, L., 2021. Comparison Between the Turbulence Parameter in the Cumulative Overload Method and the Turbulence Predictions of An OpenFOAM Model for Wave Overtopping Flow Over a Simple Dike Profile (Master Thesis). University of Twente, Water Engineering and Management, Enschede, the Netherlands.

Hewlett, H.W.M., Boorman, L.A., Bramley, L.A., 1987. Design of Reinforced Grass Waterways. Construction Industry Research and Information Association, p. 116.

Hoffmans, G.J.C.M., 2012. The Influence of Turbulence on Soil Erosion. Eburon Uitgeverij BV.

Hoffmans, G., Van Hoven, A., Steendam, G., van der Meer, J., 2018. Summary of research work about erodibility of grass revetments on dikes. In: Protections 2018 3th International Conference Against Overtopping. (June), Grange-over-Sands, UK.

Hoffmans, G., Verheij, H., 2011. Jet scour. Proc. Inst. Civ. Eng. Marit. Eng. 164 (4), 185–193. http://dx.doi.org/10.1680/maen.2011.164.4.185.

Hughes, S.A., Shaw, J.M., 2011. Continuity of instantaneous wave overtopping discharge with application to stream power concepts. J. Waterw. Port, Coast. Ocean Eng. 137 (1), 12–25. http://dx.doi.org/10.1061/(ASCE)WW.1943-5460.0000057.

Jacobsen, N.G., van Gent, M.R., Capel, A., Borsboom, M., 2018. Numerical prediction of integrated wave loads on crest walls on top of rubble mound structures. Coast. Eng. 142, 110–124. http://dx.doi.org/10.1016/j.coastaleng.2018.10.004.

Jacobsen, N.G., van Gent, M.R.A., Fredsøe, J., 2017. Numerical modelling of the erosion and deposition of sand inside a filter layer. Coast. Eng. 120, 47–63. http://dx.doi.org/10.1016/j.coastaleng.2016.09.003.

Jacobsen, N.G., van Gent, M.R., Wolters, G., 2015. Numerical analysis of the interaction of irregular waves with two dimensional permeable coastal structures. Coast. Eng. 102, 13–29. http://dx.doi.org/10.1016/j.coastaleng.2015.05.004.

Jensen, B., Jacobsen, N.G., Christensen, E.D., 2014. Investigations on the porous media equations and resistance coefficients for coastal structures. Coast. Eng. 84, 56–72. http://dx.doi.org/10.1016/j.coastaleng.2013.11.004.

Jorissen, R.E., Vrijling, J.K., 1989. Local scour downstream hydraulic constructions. In: Proceedings of the 23rd IAHR World Congress. Ottawa, Canada.

Marijnissen, R., Kok, M., Kroeze, C., van Loon-Steensma, J., 2019. Re-evaluating safety risks of multifunctional dikes with a probabilistic risk framework. Nat. Hazards Earth Syst. Sci. 19 (4), 737–756. http://dx.doi.org/10.5194/nhess-2018-295.

Molines, J., Bayón, A., Gómez-Martín, M.E., Medina, J.R., 2020. Numerical study of wave forces on crown walls of mound breakwaters with parapets. J. Mar. Sci. Eng. 8 (4), http://dx.doi.org/10.3390/JMSE8040276.

Morris, M., Benahmed, N., Philippe, P., Royet, P., Tourment, R., van den Ham, G., 2014. FloodProBE Project WP 3: Reliability of Urban Flood Defences. D3.1 Guidance on Improved Performance of Urban Flood Defences. Technical Report, FloodProBE Consortium, p. 102.

Nash, J.E., Sutcliffe, J.V., 1970. River flow forecasting through conceptual models part I-a discussion of principles*. J. Hydrol. 10, 282–290. http://dx.doi.org/10.1016/0022-1694(70)90255-6.

Nezu, I., Nakagawa, H., 1993. Turbulence in Open-Channel Flows. Taylor & Francis.

Nikuradse, J., 1950. Laws of Flow in Rough Pipes. Technical Report Technical Memorandum 1292, National Advisory Committee for Aeronautics, Washington, US, http://dx.doi.org/10.1016/s0016-0032(40)90670-6.

OpenCFD Ltd, 2019. OpenFOAM user guide.

Paarlberg, A.J., Dohmen-Janssen, C.M., Hulscher, S.J.M.H., Termes, P., 2007. A parameterization of flow separation over subaqueous dunes. Water Resour. Res. 43 (12), 12417. http://dx.doi.org/10.1029/2006WR005425.

Peeters, P., de Vos, L., Vandevoorde, B., Taverniers, E., Mostaert, F., 2012. Stabiliteit Van De Grasmat Bij Golfoverslag: Golfoverslagproeven Tielrodebroek (In Dutch). Technical Report, 713_15b, Waterbouwkundig Laboratorium, INBO en afdeling Geotechniek, Antwerp, Belgium.

Ponsioen, L., van Damme, M., Hofland, B., Peeters, P., 2019. Relating grass failure on the landside slope to wave overtopping induced excess normal stresses. Coast. Eng. 148, 49–56. http://dx.doi.org/10.1016/j.coastaleng.2018.12.009.

SBW, 2012. In: Steendam, G.J., Hoffmans, G., Jan Bakker, J., van der Meer, J.F., Paulissen, M., Verheij, H. (Eds.), Wave Overtopping and Grass Cover Strength. Model Development. Sterkte En Belastingen Waterkeren, Deltares Report (2012) 120616-007, Deltares, Delft, The Netherlands.

Scheres, B., Schüttrumpf, H., 2020. Investigating the erosion resistance of different vegetated surfaces for ecological enhancement of sea dikes. J. Mar. Sci. Eng. 8 (519), 19.

Simm, J., Ballard, B.W., Flikweert, J.-J., Maren, E.V., Dimakapoulos, A., Kinnear, R., Arthur, M., Tourment, R., Neutz, C., Steeg, P.V., 2021. Investigation, assessment and remediation of levee transitions. In: FLOODrisk 2020-4th European Conference on Flood Risk Management. Budapest University of Technology and Economics (BME), Budapest, Hungary, http://dx.doi.org/10.3311/FLOODRisk2020.14.6.

Simm, J., Flikweert, J., Hollingsworth, C., Tarrant, O., 2017. Ten years of lessons learned from english levee performance during severe flood events. In: ICOLD 2017-85th Annual Meeting of International Commission on Large Dams. Prague, Czech Republic.

Slomp, R., Knoeff, H., Bizzarri, A., Bottema, M., De Vries, W., 2016. Probabilistic flood defence assessment tools. In: E3S Web of Conferences. Vol. 7. pp. 1–14. http://dx.doi.org/10.1051/e3sconf/20160703015.

Stanczak, G., 2008. Breaching of Sea Dikes Initiated from the Seaside by Breaking Wave Impacts (Ph.D. thesis). University of Braunschweig, Faculty of Architecture, Civil Engineering and Environmental Sciences, and University of Florance, Faculty of Engineering, Braunschweig, Germany.

Steendam, G.J., Van Hoven, A., Van der Meer, J.W., Hoffmans, G., 2014. Wave overtopping simulator tests on transitions and obstacles at grass-covered slopes of dikes. Coast. Eng. Proc. 1 (34), http://dx.doi.org/10.9753/icce.v34.structures.79.

Suzuki, T., Altomare, C., Yasuda, T., Verwaest, T., 2020. Characterization of overtopping waves on sea dikes with gentle and shallow foreshores. J. Mar. Sci. Eng. 8 (10), 1–16. http://dx.doi.org/10.3390/jmse8100752.

Toimil, A., Losada, I.J., Nicholls, R.J., Dalrymple, R.A., Stive, M.J., 2020. Addressing the challenges of climate change risks and adaptation in coastal areas: A review. Coast. Eng. 156, 103611. http://dx.doi.org/10.1016/j.coastaleng.2019.103611.

USACE, 1984. The Shore Protection Manual Volume 2. Vol. II. Technical Report, U.S. Army Engineer Research and Development Center, Vicksburg, Missipi, US, http://dx.doi.org/10.5962/bhl.title.47830.

Van Bergeijk, V.M., Verdonk, V.A., Warmink, J.J., Hulscher, S.J.M.H., 2021a. The cross-dike failure probability by wave overtopping over grass-covered and damaged dikes. Water 13 (5), 690. http://dx.doi.org/10.3390/w13050690.

Van Bergeijk, V.M., Warmink, J.J., Frankena, M., Hulscher, S.J.M.H., 2019a. Modelling dike cover erosion by overtopping waves: The effects of transitions. In: Goseberg, Nils; Schlurmann, T. (Ed.), Coastal Structures 2019. Karlsruhe: Bundesanstalt für Wasserbau, pp. 1097–1106.

Van Bergeijk, V.M., Warmink, J.J., Hulscher, S.J.M.H., 2020. Modelling the wave overtopping flow over the crest and the landward slope of grass-covered flood defences. J. Mar. Sci. Eng. 8 (7), 489. http://dx.doi.org/10.3390/jmse8070489.

Van Bergeijk, V.M., Warmink, J.J., Hulscher, S.J.M.H., 2021b. Experimental Set-Up and Modelling Tools for the Load by Overtopping Waves in Erosion Models. Technical Report, University of Twente, Enschede, The Netherlands.

Van Bergeijk, V.M., Warmink, J.J., Hulscher, S.J.M.H., 2022. The wave overtopping load on landward slopes of grass-covered flood defences: Deriving practical formulations using a numerical model. Coast. Eng. 171 (104047), http://dx.doi.org/10.1016/j.coastaleng.2021.104047.

Van Bergeijk, V.M., Warmink, J.J., Van Gent, M.R.A., Hulscher, S.J.M.H., 2019b. An analytical model of wave overtopping flow velocities on dike crests and landward slopes. Coast. Eng. 149, 28–38. http://dx.doi.org/10.1016/j.coastaleng.2019.03.001.

Van Damme, M., Ponsioen, L., Herrero, M., Peeters, P., 2016. Comparing overflow and wave-overtopping induced breach initiation mechanisms in an embankment breach experiment. In: E3S Web of Conferences. Vol. 7. pp. 1–9. http://dx.doi.org/10.1051/e3sconf/20160703004.

Van Der Meer, J.W., Hardeman, B., Steendam, G.J., Schüttrumpf, H., Verheij, H., 2010. Flow depths and velocities at crest and landward slope of a dike, in theory and with the wave overtopping simulator. Coast. Eng. Proc. 1 (32), 10.

Van Der Meer, J.W., Hoffmans, G., Van Hoven, A., 2015. WTI Onderzoek En Ontwikkeling Landelijk Toetsinstrumentarium, Product 5.12 Analyses Grass Erosion in Wave Run-Up and Wave Overtopping Conditions. Deltares Report 1209437-005-HYE-0003, Deltares, Delft, The Netherlands.

Van Der Meer, J.W., Snijders, W., Regeling, E., 2007. The wave overtopping simulator. In: Coastal Engineering 2006. Vol. 5. pp. 4654–4666.

Van Doorslaer, K., Romano, A., De Rouck, J., Kortenhaus, A., 2017. Impacts on a storm wall caused by non-breaking waves overtopping a smooth dike slope. Coast. Eng. 120, 93–111. http://dx.doi.org/10.1016/J.COASTALENG.2016.11.010.

Van Hoven, A., Boers, M., 2019. BOI Omgaan Met Overgangen Bij Faalmechanisme Gras Erosie Kruin En Binnentalud, Korte Studie Naar Kansverdelingen Van Het Kritisch Overslagdebiet Inclusief Overgangen (In Dutch). Technical Report, Deltares, Delft, The Netherlands.

Van Hoven, A., Klerk, W.J., 2021. Gras Op Zand Onderzoek Product 8: Analyse Golfklapproeven En Golfoverslagproeven (In Dutch). Technical Report, 11204369-002-GEO-0015, Deltares, Delft, The Netherlands.

Van Hoven, A., Verheij, H., Hoffmans, G., Van der Meer, J., 2013. Evaluation and Model Development: Grass Erosion Test at the Rhine Dike. Technical Report, 1207811-002, Deltares, Delft, The Netherlands.

Van Loon-Steensma, J.M., Vellinga, P., 2014. Robust, multifunctional flood defenses in the dutch rural riverine area. Nat. Hazards Earth Syst. Sci. 14 (5), 1085–1098. http://dx.doi.org/10.5194/NHESS-14-1085-2014.

Van Steeg, P., van Hoven, A., 2013. Overgangen Bij Grasbekledingen in Primaire Waterkeringen (In Dutch). Technical Report, Deltares, Delft, The Netherlands.

Van Steeg, P., Labrujere, A., Mom, R., 2015. Transition structures in grass covered slopes of primary flood defences tested with the wave impact generator. In: E-Proceedings of the 36th IAHR World Congress. The Hague, The Netherlands, pp. 1–12.

Voorendt, M., 2017. Design Principles of Multifunctional Flood Defences (Ph.D. thesis). Delft University of Technology, Delft, the Netherlands, http://dx.doi.org/10.4233/uuid:31ec6c27-2f53-4322-ac2f-2852d58dfa05.

Warmink, J.J., Van Bergeijk, V.M., Frankena, M., Van Steeg, P., Hulscher, S.J.M.H., 2020. Quantifying the influence of transitions on grass cover erosion by overtopping waves. In: Coastal Engineering Proceedings 2020. pp. 1–8. http://dx.doi.org/10.9753/icce.v36v.papers.39.